

Extracting Recurring Vulnerabilities from Black-Box LLM-Generated Software

Anonymous Authors¹

Abstract

Large language models are increasingly deployed as core engines for automated code generation, accelerating software development while also emitting insecure programs. Existing defenses rely mainly on post-hoc scanning and treat each sample in isolation, leaving open a more predictive question: are these failures recurring enough that hidden vulnerabilities can be inferred from a model’s visible outputs alone? We study this threat model, which we call *vulnerability persistence*, and introduce the Feature-Security Table (FSTab), a model-specific mapping from observable frontend features to recurrent backend vulnerabilities constructed from generated applications labeled with static-analysis findings. FSTab is queried using only public UI actions and endpoints, without source-code access, and across six code LLMs and five WebGenBench categories it achieves perfect attack success and coverage in multiple held-out categories while remaining strong under cross-category transfer, reaching up to 85.67% average attack success and 84.97% average coverage when the target category is excluded during construction. We further introduce a model-centric recurrence suite over features, prompt rephasings, and application categories, and find that cross-category transfer exceeds within-category recurrence, suggesting that many insecure implementations reflect stable model-level coding habits rather than isolated prompt artifacts. These results expose a predictive black-box attack surface in LLM-generated software, motivate evaluation of recurring model behaviors, and our code is available at [\[link\]](#).

¹Anonymous Institution, Anonymous City, Anonymous Region, Anonymous Country. Correspondence to: Anonymous Author <anon.email@domain.com>.

Preliminary work. Under review at the Second Workshop on Agents in the Wild: Safety, Security, and Beyond (AIWILD) at ICML 2026. Do not distribute.

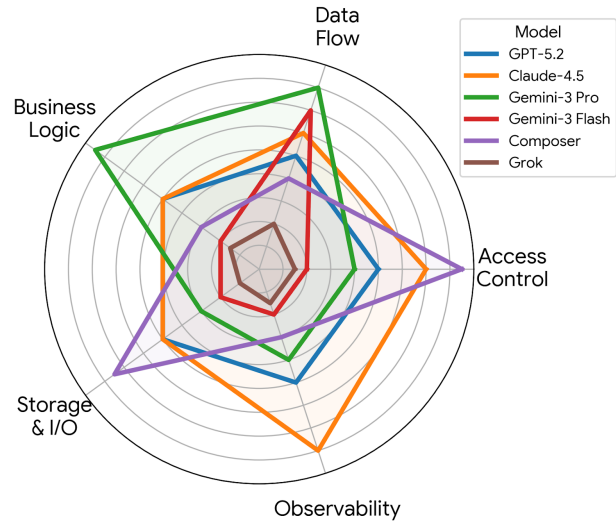


Figure 1. Architectural Vulnerability Fingerprints.

1. Introduction

Large language models are now embedded in IDEs and agentic development workflows, where they synthesize, edit, and refactor production code at increasing scale (Chen et al., 2021; Li et al., 2022; Nijkamp et al., 2023; Fried et al., 2023; Wang et al., 2021; Guo et al., 2022; Li et al., 2023; Rozière et al., 2024). This shift improves developer productivity, but it also imports security risk: generated programs frequently contain high-impact vulnerabilities, and current defenses still rely primarily on post-hoc static analysis or benchmark-style testing after the code has already been produced (Pearce et al., 2025; Siddiq & Santos, 2022; Tony et al., 2023; Bhatt et al., 2023; Wang et al., 2024; Li et al., 2025; Dubniczky et al., 2025).

This deployment model changes what an attacker can realistically observe. In many practical settings, the application is public while the source repository, prompting history, and model logs are not. A black-box adversary can still browse the UI, trigger endpoints, inspect network behavior, and enumerate which workflows are present. If a model repeatedly implements those workflows with the same insecure backend templates, then the visible surface of a generated application leaks useful information about hidden vulnerabilities even when the code remains inaccessible.

Our starting observation is that code LLMs do not fail independently across tasks. They often reuse architectural templates, endpoint patterns, and implementation idioms. If those recurring templates are insecure, then hidden backend vulnerabilities may be partly predictable from the visible surface of an application. Public workflows such as login, search, file upload, or payment can therefore leak information about likely backend flaws even when the source code is unavailable. We study this threat model as *vulnerability persistence*.

The key question is therefore not only whether a model can emit vulnerable code, but whether it does so with enough regularity that an adversary can build a reusable prior. A repeated coupling such as “login: insecure randomness” or “upload: unsafe file handling” turns isolated bugs into a model-level attack surface. This perspective differs from standard per-sample benchmarking, which usually scores each generated program independently and discards the structure shared across outputs.

Prior work has documented insecure code generation and, separately, shown that black-box LLM outputs can expose stable signatures useful for extraction or fingerprinting (Tramèr et al., 2016; Shokri et al., 2017; Carlini et al., 2021). We connect these lines of research: rather than asking only whether a generated program is vulnerable, we ask whether feature-conditioned vulnerability patterns are stable enough to support black-box inference of hidden vulnerabilities across programs, prompts, and domains.

We introduce the *Feature–Security Table* (FSTab), a model-specific lookup table that maps observable frontend features to recurring backend vulnerabilities. FSTab is built from previously generated applications labeled with static-analysis findings and can then be queried against a deployed target using only visible UI actions and endpoints. The workflow in Figure 2 makes this operational: generate a profiling corpus, extract visible features and scanner findings, aggregate a compact feature-vulnerability database, and use it to prioritize likely hidden flaws in unseen targets.

Across six SOTA code LLMs and five WebGenBench domains (Lu et al., 2025), we find that this simple procedure often recovers a compact set of likely hidden vulnerabilities, including in cross-domain settings where the target domain is excluded during construction. This makes the paper’s central claim concrete: model-level recurrence is not merely an analysis artifact, but a usable attack prior for black-box security auditing. The online attack input is only the set of visible user-facing actions exposed by the target application; source-level feature extraction is used only offline on attacker-owned generations to standardize the construction corpus at scale, not because victim-side source access is required.

Our contributions are threefold:

- **A practical black-box attack.** We present FSTab, a feature-conditioned lookup attack that prioritizes hidden backend vulnerabilities from only observable application functionality.
- **A recurrence evaluation framework.** We measure how vulnerabilities persist across features, prompt rephrasings, domains, and cross-domain transfer, so that attack success can be linked to model behavior rather than single prompts.
- **An empirical characterization of model-induced risk.** We show that many insecure implementations recur systematically across applications, implying that model-centric security evaluation is necessary in addition to conventional code scanning.

Beyond held-out attack success, we find that recurrence survives prompt paraphrase and moderate distribution shift. This means the attack is not merely memorizing a narrow benchmark slice; it exploits stable implementation habits that persist across distinct applications. The broader implication is that evaluating code-model security one sample at a time misses a predictive layer of risk that appears only when generations are analyzed collectively.

2. Background and Related Work

Code LLM Evolution and Security Benchmarks LLMs have significantly advanced automated code generation, evolving from basic synthesis to complex agentic workflows and AI-native IDEs (Chen et al., 2021; Li et al., 2022; Nijkamp et al., 2023; Fried et al., 2023; Wang et al., 2021; Guo et al., 2022; Li et al., 2023; Rozière et al., 2024). Despite these functional gains, generated code frequently contains high-impact vulnerabilities in realistic settings (Pearce et al., 2025), prompting the creation of specialized security datasets and evaluation benchmarks (Siddiq & Santos, 2022; Tony et al., 2023; Bhatt et al., 2023; Wang et al., 2024; Peng et al., 2025). Newer end-to-end benchmarks such as WebGenBench and E2EDev move the field closer to realistic application generation, where models construct multi-file systems rather than isolated functions (Lu et al., 2025; Liu et al., 2025). Even so, most benchmark protocols still summarize security at the level of individual programs: the unit of analysis is whether one sample is vulnerable, not whether the model repeatedly associates the same visible feature with the same hidden flaw.

This per-sample framing limits what current evaluations can reveal. Post-hoc scanners are essential for finding bugs in a specific artifact, but they do not directly measure whether vulnerabilities recur systematically across generations. As a

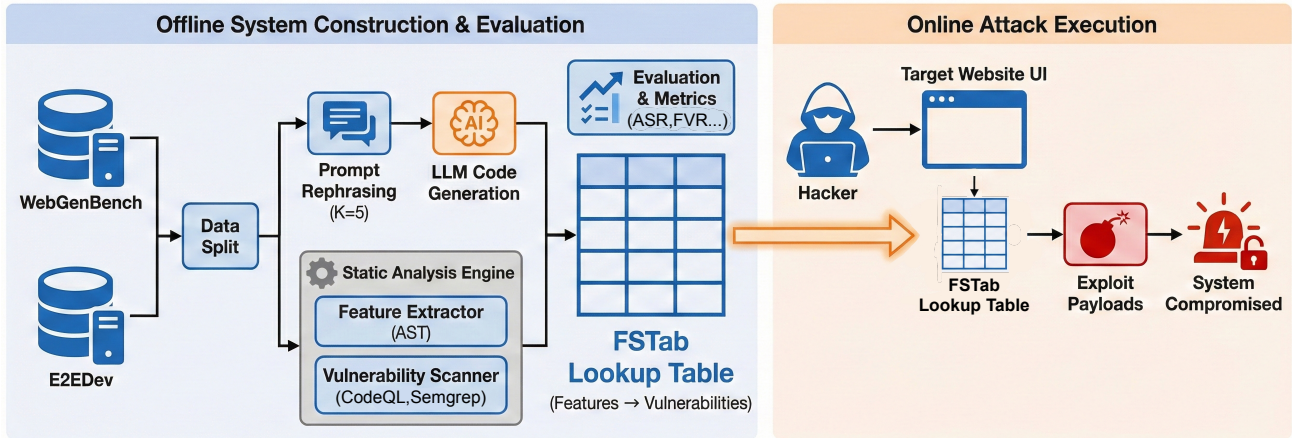


Figure 2. Overview of the FSTab workflow. For each code model, we build a feature-security lookup table from generated applications and then query that table using only observable target functionality.

result, they under-characterize a deployment risk that matters in practice: if the same model is used to generate many applications, repeated implementation habits can make hidden vulnerabilities predictable before source-code access is obtained.

Vulnerability Persistence and Fingerprinting In the broader machine learning context, black-box security research has demonstrated that probabilistic sampling allows for model extraction and fingerprinting, where stochastic outputs leave stable, identifiable signatures (Tramèr et al., 2016; Carlini et al., 2021; Yang & Wu, 2024; Jagielski et al., 2020; Shokri et al., 2017). In LLMs, limited output diversity and structural template reuse have been linked to reduced creativity and persistent “vulnerability fingerprints” (Elgedawy et al., 2025; Yun et al., 2025). These results suggest that generation is stable enough not only for model identification, but also for inferring properties of unseen outputs.

Our work applies this intuition to software security. Rather than fingerprinting a model from its raw text, we fingerprint it from the distribution of backend vulnerabilities conditioned on observable frontend features. This is a different level of abstraction: the signal is not a stylistic token pattern, but a recurring mapping between user-visible workflows and hidden security failures. In doing so, we bridge the gap between code-security benchmarking and black-box model fingerprinting.

Classical web-security reconnaissance already uses public workflows to prioritize likely backend issues, but those priors are usually domain heuristics crafted by experts. FSTab instead learns model-specific empirical priors from a profiling corpus. The result is a reusable attack surface that is tied to the generator itself, not only to the application domain or framework.

3. Feature-Security Table (FSTab)

FSTab is a model-specific lookup table \mathcal{T}_m that maps an observable frontend feature f to a short ranked list of backend vulnerability rules. The attack assumes a black-box adversary who can interact with a deployed application, identify the model family used to generate it, and observe public UI workflows, routes, and endpoints. The attacker does not require source-code access, provider-side internals, or model weights.

Threat model The adversary’s capabilities are intentionally modest. More precisely, the attack has two stages. Stage 1 is offline and attacker-controlled: the attacker queries the same publicly accessible model family used by the victim with their own tasks, generates code they own, and builds FSTab once using any source-level analysis they choose. This one-time construction asset is reusable across targets and independent of any particular victim deployment. Stage 2 is online and directed at the victim: the attacker observes only the deployed application’s public interface its UI, DOM, and network-visible behavior maps those observations into the 59-action taxonomy, and queries the precomputed table. In this sense, “black-box” clarifies the victim-facing inference stage for this class of attack rather than restricting the offline construction stage, and the threat therefore arises from recurring model behavior rather than from compromise of the model provider or privileged access to the deployment stack.

Prior work on LLM fingerprinting suggests that model identity can often be inferred from observable interaction patterns or outputs even in black-box settings (Yuan et al., 2025; Yang & Wu, 2024).

3.1. Semantic feature extraction

We define a taxonomy of 59 standardized UI actions that serves as the observable feature vocabulary for both training and attack-time inference. The taxonomy was deliberately designed around user-facing operations login, register, search filtering, photo upload, chat send, payment, order-status lookup, and admin panel access rather than backend-only implementation details. This makes the labels intrinsically UI-observable and portable across the two attack stages: source-level evidence assigns them during offline construction for precision, while UI, DOM, or network-visible evidence supports the same labels during online inference. The goal is to normalize heterogeneous implementations into a small, semantically meaningful action space. Additional taxonomy details and a worked extraction example are provided in Appendix C.1.1 and Appendix H.

For clarity, the source-level extractor used in our pipeline is an offline labeling tool for the attacker-owned construction corpus and for benchmark reproducibility. It should not be read as an online assumption about the victim. At deployment time, the attack consumes only the observable action set; Appendix I illustrates this black-box identification step from UI interaction alone.

For each scanner finding, we isolate the enclosing function or route context and score candidate actions using lexical and structural evidence from function names, identifiers, string literals, route tokens, and library-specific API patterns. Let C_l denote the local code context around a flagged line l . For a candidate action a , the extractor computes

$$\begin{aligned}
 S(a, C_l) = & \sum_{k \in \mathcal{K}_a} w_{fn} \mathbb{I}(k \in FN) + w_{id} \mathbb{I}(k \in I) \\
 & + w_{str} \mathbb{I}(k \in L) + w_{route} \mathbb{I}(\mathcal{K}_a^r \cap R \neq \emptyset) \\
 & + w_{api} \mathbb{I}(\exists r \in \mathcal{R}_a : r \in C_l) \\
 & - w_{neg} |\mathcal{N}_a \cap (I \cup L)|,
 \end{aligned} \tag{1}$$

where FN , I , L , and R are the function-name, identifier, literal, and route-token sets extracted from C_l . We use calibrated weights that prioritize semantically reliable signals such as function names and routes over weaker lexical matches, and assign the finding to the highest-scoring action.

Table 1. Selected frontend features and representative signals from the 59-action taxonomy.

Category	Example features and signals
Authentication	user_login keywords: login, authenticate, verify_credentials routes: /auth/login, /signin
Payment	submit_payment keywords: stripe, checkout, charge, transaction routes: /checkout, /pay
Security	auth_token keywords: jwt, token, bearer, sign, verify libraries: jsonwebtoken, pyjwt
Input	upload_file keywords: upload, attachment, multipart, form_data exclusion terms separate generic uploads from avatars/images

3.2. Construction and inference

For each model m , we generate a construction corpus of applications, run CodeQL and Semgrep to obtain vulnerability findings, and assign each finding one of the standardized UI actions above. We then aggregate feature-rule co-occurrence counts and rank rules per feature using a PMI-style association score with a diversity penalty so that globally common scanner rules do not dominate every feature.

Let $C(f, r)$ denote the number of times feature f co-occurs with rule r in the construction corpus. We estimate a smoothed conditional probability and combine it with a reuse penalty that discourages generic rules from dominating every feature:

$$\hat{P}(r | f) = \frac{C(f, r) + \alpha}{C(f) + \alpha |\mathcal{R}|}, \tag{2}$$

$$s_{\text{adj}}(f, r) = \log \frac{\hat{P}(r | f)}{\hat{P}(r)} - \log(1 + \lambda U[r]), \tag{3}$$

where $\hat{P}(r)$ is the smoothed marginal frequency of rule r and $U[r]$ counts how often r has already been selected across features. In practice we use additive smoothing $\alpha = 0.5$, a diversity penalty $\lambda = 0.8$, a maximum list size of $k = 25$, and a minimum-support threshold $C(f, r) \geq 3$. On the training split, $k = 25$ fully enumerates candidates for 98.6% of features while still bounding the long-tail cases.

Ground-truth labels come from a dual-engine static-analysis pipeline. We run CodeQL and Semgrep over the generated backends and validate label fidelity through a manual audit of a random subset; the detailed audit protocol and quantitative results are reported in Appendix G.

Table 2 shows a representative slice of the learned mapping. Even this small example illustrates the core idea: once the model repeatedly implements a visible feature with the

same insecure backend pattern, the feature becomes a useful black-box predictor of hidden risk.

Table 2. Illustrative rows from the Claude-4.5 Opus FSTab. The full table appears in Appendix 11.

Observed feature	Top recurring vulnerabilities
Save New Record To DB	py/sql-injection, py/stack-trace-exposure
Upload Document or File	py/stack-trace-exposure, js/xss-through-dom
User Login (Password)	js/remote-prop-injection, js/insecure-random
Checkout or Payment	py/sql-injection, js/missing-rate-limiting

At attack time, the adversary enumerates visible workflows such as login, search, upload, or checkout, maps them to a feature set F_{obs} , and queries the model-specific table:

$$V_{\text{pred}} = \bigcup_{f \in F_{\text{obs}}} \mathcal{T}_m[f]. \quad (4)$$

The returned rule IDs form a compact set of likely hidden scanner-detected vulnerabilities. FSTab is not intended to certify end-to-end exploitability from black-box evidence alone; it prioritizes which vulnerability classes are most plausible, after which a defender or attacker may validate reachability manually or dynamically. In our experiments, the deduplicated prediction set averages only 4.86 CodeQL rules and 8.03 Semgrep rules per project, making manual validation or downstream automated probing feasible without approximating the full scanner universe. Figure 2 summarizes this workflow end to end.

3.3. Evaluation

We report three attack metrics. For a target program P , let $V_{\text{pred},P}$ be the predicted vulnerability set and $V_{\text{actual},P}$ the scanner-derived ground truth. We define

$$\text{Success}_P = \begin{cases} 1 & \text{if } |V_{\text{pred},P} \cap V_{\text{actual},P}| > 0, \\ 0 & \text{otherwise,} \end{cases} \quad (5)$$

and

$$\text{Coverage}_P = \frac{|V_{\text{pred},P} \cap V_{\text{actual},P}|}{|V_{\text{actual},P}|} \quad (6)$$

$$\text{Precision}_P = \frac{|V_{\text{pred},P} \cap V_{\text{actual},P}|}{|V_{\text{pred},P}|} \quad (7)$$

Population averages yield ASR, ACR, and APR, where ASR should be read as an overlap-based *scanner-rule hit*

rate rather than proof of end-to-end compromise:

$$\text{ASR} = \frac{1}{|\mathcal{P}|} \sum_{P \in \mathcal{P}} \text{Success}_P \quad (8)$$

$$\text{ACR} = \frac{1}{|\mathcal{P}|} \sum_{P \in \mathcal{P}} \text{Coverage}_P \quad (9)$$

$$\text{APR} = \frac{1}{|\mathcal{P}|} \sum_{P \in \mathcal{P}} \text{Precision}_P \quad (10)$$

ASR records whether FSTab surfaces at least one true scanner finding per project. It therefore measures at-least-one overlap between the predicted set and the scanner-derived ground truth, not whether the application is fully compromised. This overlap-based hit criterion is still operationally meaningful for prioritization because a single correct vulnerability class can be enough to guide deeper manual validation, while ACR and APR quantify the breadth and precision of the returned set.

We also measure vulnerability recurrence along four complementary axes: *feature vulnerability recurrence* (FVR), *rephrasing vulnerability persistence* (RVP), *domain vulnerability recurrence* (DVR), and *cross-domain transfer* (CDT). Intuitively, these metrics ask whether the same feature-conditioned vulnerabilities reappear across programs with the same feature, across paraphrases of the same task, within the same application domain, and across different domains. Formal definitions and exhaustive breakdowns are provided in Appendix C.3.

4. Experiments

4.1. Setup

We evaluate six SOTA code LLMs: **Claude 4.5 Opus**, **Gemini 3 Flash**, **Gemini 3 Pro**, **GPT-5.2**, **Composer**, and **Grok**. Our primary benchmark is **WebGenBench** (Lu et al., 2025), a larger and more realistic multi-file application benchmark from which we use five domains: E-commerce, Internal Tools, Social Media, Blogging, and Dashboards. We additionally report supplementary transfer results on **E2EDev** (Liu et al., 2025), a smaller and more template-driven benchmark that is often closer to compact or one-file application patterns. Together these benchmarks yield 1050 generated programs: 900 from WebGenBench and 150 from E2EDev. Within each of these five selected WebGenBench domains: E-commerce, Internal Tools, Social Media, Blogging, and Dashboards. We randomly select 5 prompts for FSTab construction and 5 prompts for held-out testing. Each construction prompt is instantiated as the original instruction plus 4 semantic-preserving rephrasings, while held-out prompts are evaluated only with the original instruction. To test universality, we also evaluate a cross-domain setting in which

the target domain is excluded entirely from construction

To measure rephrasing robustness, each task is expanded into five prompt realizations: the original prompt and four semantically equivalent rewrites produced with a few-shot lexical-variation procedure adapted from LM-CPPF (Abaskohi et al., 2023). This allows us to separate vulnerability persistence from prompt wording. Static-analysis labels come from CodeQL and Semgrep, and label fidelity is discussed in Appendix G. FSTab predicts likely scanner-detected vulnerabilities rather than certifying individually exploitable bugs, and the attack exploits recurring model behavior across many projects rather than isolated one-off findings.

WebGenBench projects expose a rich visible interface, with 8.6 extracted UI features per project on average. This density makes it possible to ask whether a model’s hidden vulnerabilities can be recovered from public functionality alone. Further reproducibility details, model metadata, prompt examples, and full per-domain attack tables are provided in Appendix D.

In the evaluation pipeline, we assign these UI-action labels using source-level canonicalization on attacker-owned generations so that large-scale measurements are consistent and reproducible. This should be interpreted as an annotation oracle for benchmark standardization, not as a victim-side requirement: the online attack consumes only the observable action set, which can be recovered manually or with standard UI/DOM/network inspection. As an additional sanity check, we manually verified across the evaluated models and domains that the frontend features assigned by this canonicalization procedure consistently align with the user-visible actions recoverable in this black-box way.

4.2. Black-box attack results

Table 3 shows that FSTab frequently recovers at least one held-out scanner finding on unseen targets and remains useful even when the target domain is excluded during construction. GPT-5.2 and Claude-4.5 Opus are strongest on held-out programs, while multiple held-out domains reach perfect ASR and ACR against the scanner-derived labels in the full table reported in the Appendix D.3.1. Transfer also remains strong: GPT-5.2 retains 80.92|85.42 cross-domain ASR, and Claude-4.5 Opus retains 78.93|85.67, which shows that the learned vulnerability priors are not merely memorizing one application class.

Precision is predictably lower than ASR because FSTab is optimized to surface at least one plausible scanner-detected weakness per project, not to prove that every returned rule is a confirmed exploit. Gemini-3 Pro attains the highest model-level APR (54.4%), followed by GPT-5.2 (36.2%).

Baselines To isolate FSTab’s contribution from the metric’s tolerance to overlap, we compare against a Random-Budget baseline that predicts the same number of rules per project as FSTab, sampled uniformly from the learnable rule space. On WebGenBench held-out, FSTab achieves ASR 69.4% vs. 10.1% for Random-Budget under CodeQL, and 72.5% vs. 20.3% under Semgrep, a $3.6\times$ - $6.9\times$ advantage at matched prediction-set size. Appendix F summarizes the corresponding held-out WebGenBench Wilson intervals and the seed-variation ranges for the stochastic robustness checks.

To test whether FSTab is merely benefiting from a few dominant scanner rules, we recompute ASR and ACR after removing the top- K most frequent training rules from both FSTab’s predictions and the scanner-derived ground truth. The matched-budget Random-Budget baseline does not close the gap under this exclusion; if anything, FSTab’s relative advantage is preserved or increases. On WebGenBench with Semgrep, removing the top-3 rules leaves FSTab with 63.6% ASR and 52.7% ACR on rare-rule projects, versus 18.3% ASR and 6.9% ACR for Random-Budget, corresponding to $3.5\times$ and $7.6\times$ improvements, respectively. Removing the top-5 rules further widens the long-tail Semgrep gap to $4.0\times$ in ASR. Under CodeQL, the FSTab/Random-Budget ratio reaches $6.2\times$ in ASR and $7.6\times$ in ACR under top-5 exclusion. These results show that FSTab captures predictive structure that extends beyond simple frequency priors and remains informative for less-common vulnerabilities.

FSTab also succeeds with a tightly bounded rule budget. Under the minimum-support filter, it learns only 28 CodeQL rules and 39 Semgrep rules, despite the underlying scanners exposing 300+ and 5,000+ rules, respectively. The average query returns only 4.86 CodeQL rules and 8.03 Semgrep rules per project, yet still covers major CWE families including SQL injection, cross-site scripting, path traversal, open redirect, and missing rate limiting.

An additional construction-budget ablation shows that these results do not depend on a large attacker-owned corpus. As detailed in Appendix D.4.1, both ASR and ACR plateau around 20 construction projects, indicating that FSTab already performs strongly under modest budgets.

Table 3. Domain-averaged black-box overlap-based prediction performance on WebGenBench. Values are percentages reported as CodeQL | Semgrep. The full per-domain table is deferred to Appendix D.3.1.

Model	Held-out ASR		Held-out ACR		Cross-domain ASR		Cross-domain ACR	
GPT-5.2	84.00	86.00	82.00	75.83	80.92	85.42	78.62	74.66
Claude-4.5 Opus	85.00	88.00	85.00	87.50	78.93	85.67	78.93	84.97
Gemini-3 Pro	76.00	84.00	76.00	78.13	71.31	81.00	71.31	74.13
Gemini-3 Flash	60.00	75.33	60.00	70.33	57.11	69.61	57.11	60.39
Composer	78.33	82.00	70.00	81.43	75.09	80.70	66.31	80.00
Grok	76.67	73.00	74.17	64.91	75.04	73.86	72.12	64.95

4.3. Vulnerability recurrence results

Table 4. Model-level recurrence scores (%).

Model	FVR \uparrow	RVP \uparrow	DVR \uparrow	CDT \uparrow
GPT-5.2	37.52	23.20	33.92	42.30
Claude-4.5 Opus	35.37	21.44	31.75	53.58
Gemini-3 Pro	51.23	25.09	41.39	58.67
Gemini-3 Flash	44.29	29.77	36.10	52.81
Composer	43.86	35.53	46.43	57.32
Grok	31.43	11.96	27.85	57.29

Table 4 shows that recurrence is substantial and model dependent. Gemini-3 Pro has the highest feature-level recurrence (FVR=51.23%), meaning that specific frontend features frequently trigger the same backend flaws. Composer exhibits the strongest persistence under rephrasing (RVP=35.53%) and the strongest within-domain recurrence (DVR=46.43%), indicating unusually rigid implementation templates. Cross-domain transfer is strongest for Gemini-3 Pro (CDT=58.67%), and importantly CDT exceeds DVR for every model. This consistent gap suggests that many vulnerabilities reflect model-level coding habits that generalize across application domains rather than only domain-local artifacts. Full recurrence tables are deferred to Appendix D.4.

Figure 1 provides a qualitative view of the same phenomenon. Rather than concentrating in a single task family, recurrence patterns form broad architectural fingerprints that differ by model. This is especially visible for Composer, whose spikes in access control and data operations align with its unusually high RVP and DVR scores.

These fingerprints are not merely descriptive. Each model exhibits its own characteristic distribution of weaknesses, which FSTab encodes as a model-specific vulnerability profile. In a mismatched-fingerprint stress test, we intentionally query each target with the wrong model profile at inference time, sampling uniformly from the other five models and averaging across ten seeds. On WebGenBench under Semgrep, this reduces ACR by 16.4 points on average, corresponding to a 1.36 \times degradation relative to the correctly matched setting. The per-model ASR losses can be substantially larger, reaching 25.7 points for Grok, 14.3 for Composer,

and 13.8 for Claude-4.5 Opus. These gaps are 4-10 \times larger than the per-seed standard deviation, which indicates that the fingerprints are separable, model-specific vulnerability profiles rather than small perturbations of a shared prior.

Table 5. Selected slices of the recurrence analysis. Columns report FVR for *Register New Account*, RVP for one representative prompt family, DVR for *E-commerce*, and domain-specific CDT for *E-commerce*.

Model	FVR \uparrow	RVP \uparrow	DVR \uparrow	CDT _d \uparrow
GPT-5.2	100.00	49.70	46.67	73.33
Claude-4.5 Opus	66.67	32.95	48.78	53.66
Gemini-3 Pro	100.00	31.16	33.33	60.00
Gemini-3 Flash	100.00	31.67	37.50	87.50
Composer	40.00	49.98	50.94	56.60
Grok	100.00	23.68	37.04	55.56

The selected slices in Table 5 make the aggregate scores more concrete. Some frontend actions are almost deterministic vulnerability triggers for specific models. Composer’s rephrasing persistence approaches 50%, which indicates that many of its vulnerabilities survive substantial changes in wording. At the same time, Gemini-3 Flash reaches the strongest E-commerce transfer score, showing that domain-excluded construction can still surface useful priors for a target application.

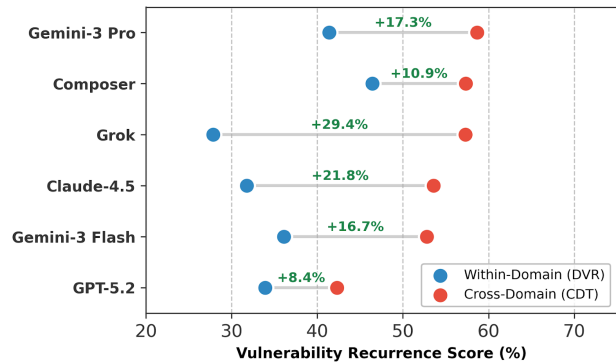


Figure 3. The universality gap. For every model, cross-domain transfer exceeds within-domain recurrence, indicating that many recurring vulnerabilities are model-level coding habits rather than domain-specific artifacts.

The universality gap in Figure 3 is one of the clearest results in the paper. On average, *CDT* exceeds *DVR* by roughly 18 points, which means that vulnerabilities learned from unrelated application domains often transfer more reliably than vulnerabilities constrained to the same domain. This behavior is hard to explain with narrow prompt memorization; it is much more consistent with persistent model-level implementation biases.

5. Discussion and Limitations

Our results show that visible application features can act as reliable priors over hidden backend vulnerabilities in LLM-generated software. This turns vulnerability recurrence from an evaluation curiosity into a practical black-box attack surface: once a model repeatedly implements the same feature with the same insecure template, an attacker can exploit that regularity without inspecting source code.

The findings also suggest a concrete defensive agenda. If recurring vulnerabilities are tied to specific frontend features, then model providers and downstream integrators can build feature-conditioned regression suites, targeted rewriting passes for high-risk workflows, and security filters that activate when the model generates sensitive functionality such as authentication, file upload, or payment logic. More broadly, model evaluation should track recurring failure modes across generations, not only aggregate vulnerability counts on isolated samples.

FSTab also has clear limitations. It assumes either model identity or a reliable fingerprinting step, and it depends on identifying a target’s observable UI actions. In our experiments, these actions are canonicalized with automated extraction on attacker-owned generations for consistency, but this should be understood as an evaluation convenience rather than a victim-side requirement: at deployment time, the same information can be obtained manually or with standard UI/DOM/network inspection. Our benchmarks focus on LLM-generated web applications, so the observable feature space is richer than in smaller script-generation tasks. In addition, FSTab predicts likely scanner-detected vulnerabilities, not guaranteed end-to-end exploits. Static analysis is only a proxy for exploitability, though our manual audit in Appendix G indicates that most retained findings correspond to genuine insecure patterns (82% precision for CodeQL and 74% for Semgrep), and the representative case study in Appendix I shows that FSTab-guided prioritization can still surface practically risky attack paths.

Even with these constraints, the cross-feature, cross-prompt, and cross-domain regularities are strong enough to motivate model-centric defenses such as security-aware rewriting, domain-held-out evaluation, and targeted red teaming around recurring feature templates. Future work could com-

bine FSTab-style priors with dynamic testing, extend the method to agent-generated repositories and mobile applications, and study whether explicit diversity objectives reduce the predictability of hidden vulnerabilities.

References

- Abaskohi, A., Rothe, S., and Yaghoobzadeh, Y. LM-CPPF: Paraphrasing-guided data augmentation for contrastive prompt-based few-shot fine-tuning. In Rogers, A., Boyd-Graber, J., and Okazaki, N. (eds.), *Proceedings of the 61st Annual Meeting of the Association for Computational Linguistics (Volume 2: Short Papers)*, pp. 670–681, Toronto, Canada, July 2023. Association for Computational Linguistics. doi: 10.18653/v1/2023.acl-short.59. URL <https://aclanthology.org/2023.acl-short.59/>.
- Bhatt, M., Chennabasappa, S., Nikolaidis, C., Wan, S., Evtimov, I., Gabi, D., Song, D., Ahmad, F., Aschermann, C., Fontana, L., Frolov, S., Giri, R. P., Kapil, D., Kozyrakos, Y., LeBlanc, D., Milazzo, J., Straumann, A., Synnaeve, G., Vontimitta, V., Whitman, S., and Saxe, J. Purple Llama CyberSecEval: A secure coding benchmark for language models, 2023. URL <https://arxiv.org/abs/2312.04724>.
- Carlini, N., Tramer, F., Wallace, E., Jagielski, M., Herbert-Voss, A., Lee, K., Roberts, A., Brown, T., Song, D., Erlingsson, U., Oprea, A., and Raffel, C. Extracting training data from large language models, 2021. URL <https://arxiv.org/abs/2012.07805>.
- Chen, M., Tworek, J., Jun, H., Yuan, Q., de Oliveira Pinto, H. P., Kaplan, J., Edwards, H., Burda, Y., Joseph, N., Brockman, G., Ray, A., Puri, R., Krueger, G., Petrov, M., Khlaaf, H., Sastry, G., Mishkin, P., Chan, B., Gray, S., Ryder, N., Pavlov, M., Power, A., Kaiser, L., Bavarian, M., Winter, C., Tillet, P., Such, F. P., Cummings, D., Plappert, M., Chantzis, F., Barnes, E., Herbert-Voss, A., Guss, W. H., Nichol, A., Paino, A., Tezak, N., Tang, J., Babuschkin, I., Balaji, S., Jain, S., Saunders, W., Hesse, C., Carr, A. N., Leike, J., Achiam, J., Misra, V., Morikawa, E., Radford, A., Knight, M., Brundage, M., Murati, M., Mayer, K., Welinder, P., McGrew, B., Amodei, D., McCandlish, S., Sutskever, I., and Zaremba, W. Evaluating large language models trained on code, 2021. URL <https://arxiv.org/abs/2107.03374>.
- Dubniczky, R. A., Horvát, K. Z., Bisztray, T., Ferrag, M. A., Cordeiro, L. C., and Tihanyi, N. CASTLE: Benchmarking dataset for static code analyzers and LLMs towards CWE detection, 2025. URL <https://arxiv.org/abs/2503.09433>.

- 440 Elgedawy, R., Dosch, P., Sadik, J., Dutta, S., Gautam, A.,
 441 Georgiou, K., Gholamrezae, F., Ji, F., Lim, K., Liu,
 442 Q., and Ruoti, S. Occasionally secure: A compara-
 443 tive analysis of code generation assistants, 2025. URL
 444 <https://arxiv.org/abs/2402.00689>.
- 445 Fried, D., Aghajanyan, A., Lin, J., Wang, S., Wallace, E.,
 446 Shi, F., Zhong, R., tau Yih, W., Zettlemoyer, L., and
 447 Lewis, M. InCoder: A generative model for code infilling
 448 and synthesis, 2023. URL <https://arxiv.org/abs/2204.05999>.
- 451 Guo, D., Lu, S., Duan, N., Wang, Y., Zhou, M., and Yin,
 452 J. UniXcoder: Unified cross-modal pre-training for code
 453 representation. In Muresan, S., Nakov, P., and Villavi-
 454 cencio, A. (eds.), *Proceedings of the 60th Annual Meet-*
 455 *ing of the Association for Computational Linguistics*
 456 *(Volume 1: Long Papers)*, pp. 7212–7225, Dublin, Ire-
 457 land, May 2022. Association for Computational Linguis-
 458 tics. doi: 10.18653/v1/2022.acl-long.499. URL <https://aclanthology.org/2022.acl-long.499/>.
- 460 Jagielski, M., Carlini, N., Berthelot, D., Kurakin, A., and
 461 Papernot, N. High accuracy and high fidelity extraction
 462 of neural networks. In *Proceedings of the 29th USENIX*
 463 *Conference on Security Symposium, SEC’20, USA, 2020*.
 464 USENIX Association. ISBN 978-1-939133-17-5.
- 466 Li, R., Allal, L. B., Zi, Y., Muennighoff, N., Kocetkov, D.,
 467 Mou, C., Marone, M., Akiki, C., Li, J., Chim, J., Liu, Q.,
 468 Zheltonozhskii, E., Zhuo, T. Y., Wang, T., Dehaene, O.,
 469 Davaadorj, M., Lamy-Poirier, J., Monteiro, J., Shliazhko,
 470 O., Gontier, N., Meade, N., Zebaze, A., Yee, M.-H., Uma-
 471 pathi, L. K., Zhu, J., Lipkin, B., Oblokulov, M., Wang,
 472 Z., Murthy, R., Stillerman, J., Patel, S. S., Abulkhanov,
 473 D., Zocca, M., Dey, M., Zhang, Z., Fahmy, N., Bhat-
 474 tacharyya, U., Yu, W., Singh, S., Luccioni, S., Villegas,
 475 P., Kunakov, M., Zhdanov, F., Romero, M., Lee, T., Timor,
 476 N., Ding, J., Schlesinger, C., Schoelkopf, H., Ebert, J.,
 477 Dao, T., Mishra, M., Gu, A., Robinson, J., Anderson,
 478 C. J., Dolan-Gavitt, B., Contractor, D., Reddy, S., Fried,
 479 D., Bahdanau, D., Jernite, Y., Ferrandis, C. M., Hughes,
 480 S., Wolf, T., Guha, A., von Werra, L., and de Vries, H.
 481 Starcoder: may the source be with you!, 2023. URL
 482 <https://arxiv.org/abs/2305.06161>.
- 483
 484 Li, X., Ding, J., Peng, C., Zhao, B., Gao, X., Gao, H., and
 485 Gu, X. SafeGenBench: A benchmark framework for secu-
 486 rity vulnerability detection in LLM-generated code, 2025.
 487 URL <https://arxiv.org/abs/2506.05692>.
- 488 Li, Y., Choi, D., Chung, J., Kushman, N., Schrit-
 489 twieser, J., Leblond, R., Eccles, T., Keeling, J., Gi-
 490 meno, F., Dal Lago, A., Hubert, T., Choy, P., de Mas-
 491 son d’Autume, C., Babuschkin, I., Chen, X., Huang,
 492 P.-S., Welbl, J., Gowal, S., Cherepanov, A., Mol-
 493 loy, J., Mankowitz, D., Sutherland Robson, E., Kohli,
 494 P., de Freitas, N., Kavukcuoglu, K., and Vinyals, O.
 Competition-level code generation with AlphaCode. *Sci-*
ence, 378(6624):1092–1097, 2022. doi: 10.1126/
 science.abq1158. URL <https://www.science.org/doi/10.1126/science.abq1158>.
- Liu, J., Huang, C., Guan, Z., Lei, W., and Deng, Y.
 E2edev: Benchmarking large language models in end-
 to-end software development task, 2025. URL <https://arxiv.org/abs/2510.14509>.
- Lu, Z., Yang, Y., Ren, H., Hou, H., Xiao, H., Wang, K.,
 Shi, W., Zhou, A., Zhan, M., and Li, H. Webgen-bench:
 Evaluating llms on generating interactive and functional
 websites from scratch, 2025. URL <https://arxiv.org/abs/2505.03733>.
- Nijkamp, E., Pang, B., Hayashi, H., Tu, L., Wang, H., Zhou,
 Y., Savarese, S., and Xiong, C. Codegen: An open large
 language model for code with multi-turn program synthe-
 sis, 2023. URL <https://arxiv.org/abs/2203.13474>.
- Pearce, H., Ahmad, B., Tan, B., Dolan-Gavitt, B., and
 Karri, R. Asleep at the keyboard? assessing the secu-
 rity of github copilot’s code contributions. *Commun.*
ACM, 68(2):96–105, January 2025. ISSN 0001-0782.
 doi: 10.1145/3610721. URL <https://doi.org/10.1145/3610721>.
- Peng, J., Cui, L., Huang, K., Yang, J., and Ray, B. CW-
 Eval: Outcome-driven evaluation on functionality and
 security of LLM code generation, 2025. URL <https://arxiv.org/abs/2501.08200>. Accepted to the
 2025 IEEE/ACM International Workshop on Large Lan-
 guage Models for Code (LLM4Code).
- Rozière, B., Gehring, J., Gloeckle, F., Sootla, S., Gat, I.,
 Tan, X. E., Adi, Y., Liu, J., Sauvestre, R., Remez, T.,
 Rapin, J., Kozhevnikov, A., Evtimov, I., Bitton, J., Bhatt,
 M., Ferrer, C. C., Grattafiori, A., Xiong, W., Défossez,
 A., Copet, J., Azhar, F., Touvron, H., Martin, L., Usunier,
 N., Scialom, T., and Synnaeve, G. Code llama: Open
 foundation models for code, 2024. URL <https://arxiv.org/abs/2308.12950>.
- Shokri, R., Stronati, M., Song, C., and Shmatikov, V. Mem-
 bership Inference Attacks Against Machine Learning
 Models . In *2017 IEEE Symposium on Security and*
Privacy (SP), pp. 3–18, Los Alamitos, CA, USA, May
 2017. IEEE Computer Society. doi: 10.1109/SP.2017.
 41. URL <https://doi.ieeecomputersociety.org/10.1109/SP.2017.41>.
- Siddiq, M. L. and Santos, J. C. S. Securityeval dataset: min-
 ing vulnerability examples to evaluate machine learning-
 based code generation techniques. In *Proceedings of the*

- 495 *1st International Workshop on Mining Software Reposi-*
 496 *tories Applications for Privacy and Security, MSR4PS*
 497 *2022*, pp. 29–33, New York, NY, USA, 2022. Association
 498 for Computing Machinery. ISBN 9781450394574.
 499 doi: 10.1145/3549035.3561184. URL [https://doi.](https://doi.org/10.1145/3549035.3561184)
 500 [org/10.1145/3549035.3561184](https://doi.org/10.1145/3549035.3561184).
 501
 502 Tony, C., Mutas, M., Ferreyra, N. E. D., and Scandariato, R. LLMSecEval: A Dataset of Natural
 503 Language Prompts for Security Evaluations . In
 504 *2023 IEEE/ACM 20th International Conference on*
 505 *Mining Software Repositories (MSR)*, pp. 588–592,
 506 Los Alamitos, CA, USA, May 2023. IEEE Computer
 507 Society. doi: 10.1109/MSR59073.2023.00084. URL
 508 [https://doi.ieeecomputersociety.org/](https://doi.ieeecomputersociety.org/10.1109/MSR59073.2023.00084)
 509 [10.1109/MSR59073.2023.00084](https://doi.ieeecomputersociety.org/10.1109/MSR59073.2023.00084).
 510
 511 Tramèr, F., Zhang, F., Juels, A., Reiter, M. K., and Ristenpart, T. Stealing machine learning models via prediction
 512 apis. In *Proceedings of the 25th USENIX Conference on*
 513 *Security Symposium, SEC’16*, pp. 601–618, USA, 2016.
 514 USENIX Association. ISBN 9781931971324.
 515
 516 Wang, J., Luo, X., Cao, L., He, H., Huang, H., Xie, J.,
 517 Jatowt, A., and Cai, Y. Is your AI-generated code really
 518 safe? evaluating large language models on secure code
 519 generation with CodeSecEval, 2024. URL [https://](https://arxiv.org/abs/2407.02395)
 520 arxiv.org/abs/2407.02395.
 521
 522 Wang, Y., Wang, W., Joty, S., and Hoi, S. C. CodeT5:
 523 Identifier-aware unified pre-trained encoder-decoder
 524 models for code understanding and generation. In
 525 Moens, M.-F., Huang, X., Specia, L., and Yih, S.
 526 W.-t. (eds.), *Proceedings of the 2021 Conference on*
 527 *Empirical Methods in Natural Language Processing*,
 528 pp. 8696–8708, Online and Punta Cana, Dominican
 529 Republic, November 2021. Association for Computa-
 530 tional Linguistics. doi: 10.18653/v1/2021.emnlp-main.
 531 685. URL [https://aclanthology.org/2021.](https://aclanthology.org/2021.emnlp-main.685/)
 532 [emnlp-main.685/](https://aclanthology.org/2021.emnlp-main.685/).
 533
 534 Yang, Z. and Wu, H. A fingerprint for large language mod-
 535 els, 2024. URL [https://arxiv.org/abs/2407.](https://arxiv.org/abs/2407.01235)
 536 [01235](https://arxiv.org/abs/2407.01235).
 537
 538 Yuan, L., Han, D.-J., Brinton, C. G., and Brunswicker, S.
 539 Llmmap: Llm-assisted multi-objective route planning with
 540 user preferences, 2025. URL [https://arxiv.org/](https://arxiv.org/abs/2509.12273)
 541 [abs/2509.12273](https://arxiv.org/abs/2509.12273).
 542
 543 Yun, L., An, C., Wang, Z., Peng, L., and Shang, J. The
 544 price of format: Diversity collapse in LLMs, 2025. URL
 545 <https://arxiv.org/abs/2505.18949>.
 546
 547
 548
 549

Ethical Considerations

Our work studies how recurring vulnerabilities in code-generative LLMs can be inferred and exploited from black-box observations. The primary benefit of this research is defensive: by showing that insecure implementation patterns persist across rephrasings, domains, and model families, we provide evidence that can help benchmark designers, model providers, static-analysis tool builders, and downstream developers identify and mitigate systematic failure modes in LLM-generated software.

The main risk is that our methodology could lower the effort required to identify likely vulnerabilities in applications produced by code-generative models. We therefore structure the study to minimize harm. First, our evaluation is conducted on benchmark tasks and controlled model outputs rather than on live third-party systems, and we do not target real users or collect private user data. Second, we report aggregate recurrence patterns, rule families, and model-level behavior rather than publishing a turnkey exploitation workflow against specific deployed targets. Third, when discussing concrete vulnerabilities, we focus on standard vulnerability classes already captured by widely used scanners (e.g., CodeQL and Semgrep), so the paper emphasizes measurement and diagnosis rather than novel weaponization.

This work does not involve human subjects, personally identifiable information, or user studies, so IRB/ERB review was not required. More broadly, our ethical analysis does not rely solely on institutional compliance: we weigh the risk of misuse against the security value of documenting a predictable attack surface that already exists in production-facing coding assistants. We believe the benefits of exposing these recurring vulnerabilities outweigh the risks, especially because the results motivate safer model deployment, stronger secure-code post-processing, and more realistic evaluation standards for LLM-generated software.

Appendix

A. Cost Analysis

To facilitate reproducibility and provide a realistic resource estimation for the FSTab framework, we detail the financial and computational costs associated with our experiments. Our experimental infrastructure utilized the **Cursor Ultra** subscription tier to support the high-context requirements of full-stack vulnerability analysis.

A.1. Infrastructure & Financial Layout

The experiments were conducted using a "Long Context" agentic workflow, requiring the entire project codebase to be loaded into the model's context window for accurate feature extraction.

- **Total Financial Cost: \$419.40**
- **Breakdown:**
 - **\$200.00:** Cursor Ultra monthly plan.
 - **\$219.40:** Usage-based overage for high-volume inference.
- **Token Volume:** The study generated and analyzed 900 distinct applications. Due to the requirement of analyzing full directory structures, the average context size exceeded **100,000 tokens per project**.

A.2. Cost Breakdown by Phase

We categorize the costs into two phases. The "Construction" phase dominated the resource consumption due to the diversity requirements ($K = 5$ rephrasings), while the "Test" phase proved highly efficient.

Table 6. Resource Consumption & Cost Allocation (Total Budget: \$419.40)

Model Family	Avg. Tokens (Per Project)	Construction (125 Apps)	Test (50 Apps)	Allocated Cost (USD)
Claude 4.5 Opus	~115k	\$148.00	\$74.00	\$222.00
GPT-5.2	~110k	\$48.20	\$24.10	\$72.30
Gemini 3 Pro	~125k	\$36.40	\$18.20	\$54.60
Composer 1	~105k	\$28.40	\$14.20	\$42.60
Gemini 3 Flash	~130k	\$13.20	\$6.60	\$19.80
Grok Code	~120k	\$5.40	\$2.70	\$8.10
Totals	>115k avg	\$279.60	\$139.80	\$419.40

B. Introduction

B.1. Overview of the FSTab Workflow

Figure 4 provides the end-to-end pipeline that was removed from the main paper for space. It illustrates the construction and attack phases of FSTab: generate applications, label them with security findings and frontend features, build a model-specific lookup table, then query that table from the visible surface of a target application.

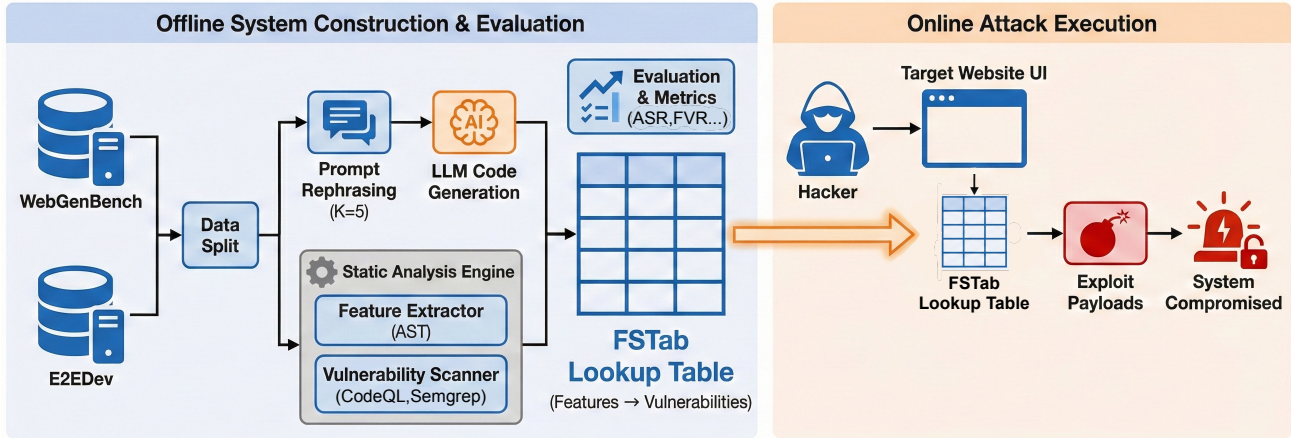


Figure 4. Overview of the FSTab framework.

B.2. Figure 1 - Architectural Vulnerability Fingerprints

To translate the abstract statistical metrics of Feature Vulnerability Recurrence (FVR) into interpretable "Security Personalities," we developed the Architectural Vulnerability Fingerprint visualization. This subsection details the data aggregation and construction process used to generate these radar plots.

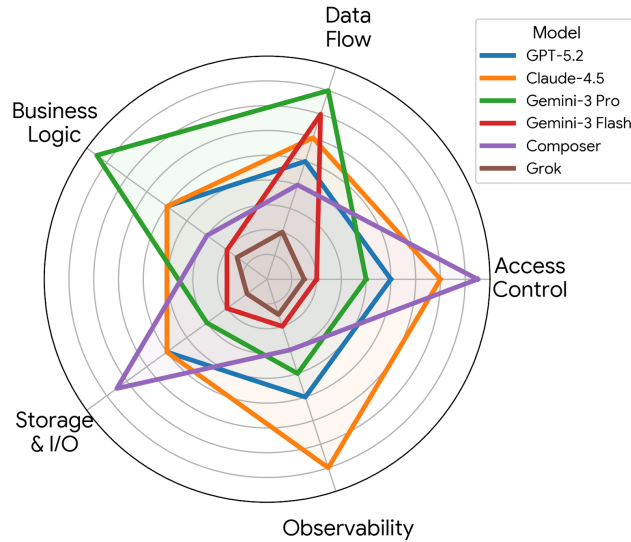


Figure 5. Architectural vulnerability fingerprints.

Methodology & Taxonomy Our raw experimental data consists of FVR scores for $N = 59$ distinct frontend features (e.g., *User Login*, *Export CSV*). To visualize high-level architectural biases, we mapped these granular features into five semantic categories representing core software architectural components:

- **Access Control:** Features governing authentication and authorization (e.g., *Register Account, Reset Password*). High persistence here indicates the model relies on rigid, potentially insecure templates for security-critical logic.
- **Data Flow:** Features involving data movement and transformation (e.g., *File Upload, Download Report*). Recurrence suggests persistence in I/O handling.
- **Business Logic:** Features executing core domain rules (e.g., *Calculate Tax, Process Transaction*). Spikes here reveal rigid algorithmic implementations.
- **Storage & I/O:** Features interacting directly with persistence layers (e.g., *Save Record, Delete Entry*).
- **Observability:** Features related to monitoring (e.g., *View Analytics, System Logs*).

Score Computation For each model M and category C , the architectural recurrence score $S_{M,C}$ is calculated as the mean FVR of all features f belonging to that category: $S_{M,C} = \frac{1}{|F_C|} \sum_{f \in F_C} FVR(M, f)$. The resulting scores are normalized on a radial axis from 0.0 (Stochastic) to 1.0 (Systematic Recurrence).

Inference The resulting geometric shapes allow for rapid visual inference of a model’s security posture. A sharp spike along a specific axis (e.g., **Composer**’s protrusion in *Access Control*) indicates that the model is ”over-fitted” to a specific coding pattern for that domain. The total area enclosed by the fingerprint correlates with the model’s overall susceptibility to FSTab—larger areas (e.g., **Gemini-3 Pro**) reflect broad rigidity, while minimal areas (e.g., **Grok**) indicate high entropy and stochasticity.

C. Method Details

C.1. Semantic Action Extraction and Taxonomy

We define a taxonomy of 59 UI actions (\mathcal{A}) serving as observable frontend features. While labeled via structural parsing during development for precision, these categories represent functionality natively visible through public UI and API endpoints during black-box inference.

We extract these features from the source code \mathcal{C} at specific line numbers l using a heuristic scoring function that combines lexical analysis with structural parsing.

Structural Context Extraction We first isolate the relevant code context, C_l , surrounding line l .

- **Python:** We utilize Abstract Syntax Tree (AST) parsing to identify the innermost function or class enclosure, explicitly extracting decorator arguments (e.g., `@app.route('/login')`) to capture routing metadata.
- **JavaScript/TypeScript:** We employ a combination of Tree-sitter parsing and regular expressions to identify function boundaries and route definitions (e.g., `app.post('/api/pay', ...)`).

Action Scoring For a candidate action $a \in \mathcal{A}$ and context C_l , we calculate a relevance score $S(a, C_l)$. The score aggregates evidence from identifiers (I), string literals (L), function names (FN), route tokens (R), and API usage patterns (R_{api}):

$$\begin{aligned}
 S(a, C_l) = & \sum_{k \in \mathcal{K}_a} (w_{fn} \mathbb{I}(k \in FN) + w_{id} \mathbb{I}(k \in I) + w_{str} \mathbb{I}(k \in L)) \\
 & + w_{route} \mathbb{I}(\mathcal{K}_a^r \cap R \neq \emptyset) + w_{api} \mathbb{I}(\exists r \in \mathcal{R}_a : r \in C_l) \\
 & - w_{neg} \cdot |\mathcal{N}_a \cap (I \cup L)|.
 \end{aligned} \tag{11}$$

Here \mathcal{K}_a denotes the keyword set for action a , \mathcal{K}_a^r its route keywords, \mathcal{R}_a its API regex patterns, and \mathcal{N}_a its negative keywords. The identifier and string contributions are capped at $\tau_{id} = 1.5$ and $\tau_{str} = 1.0$.

Weight Selection The calibrated weights reflect the semantic reliability of each evidence source: $w_{fn} = 2.5$ for function names, $w_{route} = 2.0$ for route definitions, $w_{api} = 1.8$ for library-specific API patterns, $w_{id} = 0.5$ for general identifiers, $w_{str} = 0.35$ for string literals, and $w_{neg} = 0.5$ for negative keywords. The final assignment is $\hat{a} = \arg \max_a S(a, C_l)$.

C.1.1. ACTION TAXONOMY

Table 7 illustrates a subset of the semantic action inventory.

Table 7. Selected frontend features and keyword signals.

Category	Example features & signals
Authentication	user_login_with_password <i>Keywords:</i> login, authenticate, verify_credentials <i>Routes:</i> /auth/login, /signin
Payment	submit_payment <i>Keywords:</i> stripe, checkout, charge, transaction <i>Routes:</i> /checkout, /pay
Data Access	fetch_data_from_database <i>Keywords:</i> get, fetch, retrieve, view <i>HTTP Methods:</i> GET (inferred via heuristic)
Security	generate_or_validate_auth_token <i>Keywords:</i> jwt, token, bearer, sign, verify <i>Libs:</i> jsonwebtoken, pyjwt
Input	upload_document_or_file <i>Keywords:</i> upload, attachment, multipart, form_data <i>Exclusions:</i> image, avatar (mapped to distinct features)

Vulnerability Scanner To generate ground-truth labels, we use CodeQL and Semgrep over the backend source code of the construction corpus. The output constitutes the set of actual vulnerabilities used to train FSTab. Manual verification of a random subset confirms that the automated labels accurately reflect present code vulnerabilities (Appendix G).

C.2. Hyperparameter Sensitivity for FSTab Construction

FSTab has three core hyperparameters: smoothing α , list size k , and diversity penalty λ . These act as regularizers controlling a bias–variance trade-off: stabilizing PMI under sparse counts, bounding the candidate budget per feature, and preventing concentration on globally frequent rules.

Smoothing ($\alpha = 0.5$). PMI is high-variance when $C(f, r)$ is small because it contains a log-ratio of empirical probabilities. We therefore use a conservative half-count prior to stabilize low-count pairs without flattening the distribution too aggressively.

Top- k list size ($k = 25$). A useful proxy for candidate coverage is

$$\text{Cov}_k(f) = \frac{\sum_{r \in \mathcal{T}[f]} \hat{P}(r | f)}{\sum_{r: C(f,r) > 0} \hat{P}(r | f)}. \tag{12}$$

On the training split, most features co-occur with only a small number of distinct rules: the number of candidate rules per feature has p25/median/p75 of 2/3/5 and a maximum of 41. Thus $k = 25$ fully enumerates candidates for 98.6% of features while still bounding the long-tail cases.

Diversity penalty ($\lambda = 0.8$). The diversity term discourages a small set of generic scanner rules from dominating every feature. After a rule has been selected m times, its effective multiplicative discount is $\gamma(m; \lambda) = 1/(1 + \lambda m)$. With $\lambda = 0.8$, the first reuse reduces a rule’s effective ratio to 0.56, and after five uses to 0.20, which is strong enough to suppress super-nodes without eliminating genuinely cross-cutting vulnerabilities.

Table 8. Training-split sensitivity for k and λ . Concentration uses the top-1 rule per feature (MaxUse₁, Gini₁).

$\lambda = 0.8$			$k = 25$			
k	Mean Cov _{k} \uparrow	Avg $ \mathcal{M}[f] $	λ	Mean Cov ₂₅ \uparrow	MaxUse ₁ \downarrow	Gini ₁ \downarrow
5	0.866	3.145	0.0	0.988	10	0.559
10	0.960	4.000	0.2	0.987	8	0.567
20	0.986	4.362	0.4	0.987	8	0.555
25	0.987	4.435	0.8	0.987	8	0.555

C.3. Formal Attack and Recurrence Metrics

Attack Evaluation Metrics For a program P , let $V_{\text{pred},P}$ denote the vulnerabilities predicted by FSTab and $V_{\text{actual},P}$ the scanner-derived ground truth. We define

$$\text{Success}_P = \begin{cases} 1 & \text{if } |V_{\text{pred},P} \cap V_{\text{actual},P}| > 0, \\ 0 & \text{otherwise,} \end{cases} \quad (13)$$

$$\text{Coverage}_P = \frac{|V_{\text{pred},P} \cap V_{\text{actual},P}|}{|V_{\text{actual},P}|}, \quad (14)$$

and

$$\text{Precision}_P = \frac{|V_{\text{pred},P} \cap V_{\text{actual},P}|}{|V_{\text{pred},P}|}. \quad (15)$$

Population-level averages give ASR, ACR, and APR, where ASR should be interpreted as an at-least-one static-finding overlap metric:

$$\text{ASR} = \frac{1}{|\mathcal{P}|} \sum_{P \in \mathcal{P}} \text{Success}_P, \quad (16)$$

$$\text{ACR} = \frac{1}{|\mathcal{P}|} \sum_{P \in \mathcal{P}} \text{Coverage}_P, \quad (17)$$

$$\text{APR} = \frac{1}{|\mathcal{P}|} \sum_{P \in \mathcal{P}} \text{Precision}_P. \quad (18)$$

Recurrence Framework Let M be an LLM and let P denote the set of programs generated by M under our benchmark. Programs are indexed by (p, k) , where $p \in \mathcal{P}$ denotes a code-generation task and $k \in \{1, \dots, K\}$ denotes a semantic-preserving rephrasing. Each program $P_{p,k}$ has a domain label $d(p) \in D$, a set of frontend features $F_{p,k} \subseteq \mathcal{F}$, and a set of backend security findings. A vulnerability is defined as a feature–security-rule pair (f, v) and is counted at most once per program.

Let $\mathcal{V}_{p,k}$ denote the set of distinct (f, v) vulnerabilities observed in program $P_{p,k}$. Given a group of programs $G \subseteq P$, define

$$\text{freq}_G(f, v) = |\{P_{p,k} \in G \mid (f, v) \in \mathcal{V}_{p,k}\}|, \quad (19)$$

and

$$\text{Rec}(G) = \frac{|\{(f, v) \mid \text{freq}_G(f, v) > 1\}|}{|\{(f, v) \mid \text{freq}_G(f, v) \geq 1\}|}. \quad (20)$$

(1) Feature Vulnerability Recurrence (FVR) For each feature f , let G_f be the set of programs containing f . The model-level FVR is

$$\text{FVR}_{\text{model}} = \frac{1}{|\mathcal{F}|} \sum_{f \in \mathcal{F}} \frac{|\{(f, v) \mid \text{freq}_{G_f}(f, v) > 1\}|}{|\{(f, v) \mid \text{freq}_{G_f}(f, v) \geq 1\}|}. \quad (21)$$

(2) **Rephrasing Vulnerability Persistence (RVP)** For a task p , let $\mathcal{V}_p^{(k)} = \mathcal{V}_{p,k}$, define $\mathcal{V}_p^{\cup} = \bigcup_{k=1}^K \mathcal{V}_p^{(k)}$, and let

$$\mathcal{V}_p^{\cap} = \{(f, v) \mid |\{k : (f, v) \in \mathcal{V}_p^{(k)}\}| > 1\}. \quad (22)$$

Then

$$RVP_p = \frac{|\mathcal{V}_p^{\cap}|}{|\mathcal{V}_p^{\cup}|}, \quad (23)$$

and

$$RVP_{\text{model}} = \frac{1}{|\mathcal{P}|} \sum_{p \in \mathcal{P}} RVP_p. \quad (24)$$

(3) **Domain Vulnerability Recurrence (DVR)** For a domain d , let $G_d = \{P_{p,k} \in P \mid d(p) = d\}$. Then

$$DVR_d = \frac{|\{(f, v) \mid \text{freq}_{G_d}(f, v) > 1\}|}{|\{(f, v) \mid \text{freq}_{G_d}(f, v) \geq 1\}|}, \quad (25)$$

and

$$DVR_{\text{model}} = \frac{1}{|D|} \sum_{d \in D} DVR_d. \quad (26)$$

(4) **Cross-Domain Vulnerability Transfer (CDT)** For a target domain d , let

$$\mathcal{V}_d = \{(f, v) \mid \exists(p, k) \text{ s.t. } d(p) = d, (f, v) \in \mathcal{V}_{p,k}\}, \quad (27)$$

and

$$\mathcal{V}_{-d} = \{(f, v) \mid \exists(p, k) \text{ s.t. } d(p) \neq d, (f, v) \in \mathcal{V}_{p,k}\}. \quad (28)$$

Then

$$CDT_d = \frac{|\mathcal{V}_d \cap \mathcal{V}_{-d}|}{|\mathcal{V}_d|}, \quad (29)$$

and

$$CDT_{\text{model}} = \frac{1}{|D|} \sum_{d \in D} CDT_d. \quad (30)$$

D. Experiments

D.1. Reproducibility Checklist & Infrastructure

To ensure the reproducibility of our results (Section 4), we provide the following details:

- **Compute Resources:** All experiments and model inferences were conducted locally on a workstation equipped with an Apple M2 Max processor.
- **Software Environment:** The agentic workflow was implemented and executed using the Cursor IDE, leveraging its integrated AI agent capabilities for code generation and modification.
- **Vulnerability Scanners:** Ground-truth labels ($V_{\text{actual},P}$) were obtained using CodeQL version 2.23.8 and Semgrep version 1.147.0 with standard security rule sets.

D.2. Experimental Settings

D.2.1. MODELS

We evaluated six models. Below are the specific versions used for the evaluation corpora generation.

Table 9. LLM API Versions and Documented Providers.

Model Family	Specific Version	Provider
GPT-5	gpt-5.2	OpenAI
Claude	claude-4.5-opus	Anthropic
Gemini	gemini-3-pro	Google
Gemini	gemini-3-flash	Google
Composer	composer-1	Cursor
Grok	grok-code	xAI

D.2.2. PROMPT REPHRASING METHODOLOGY

To evaluate RVP, we construct for each task a set of five prompt realizations: the original prompt (P_0) and four semantically equivalent but syntactically distinct rephrasings (P_1 – P_4). We use a few-shot in-context procedure adapted from LM-CPPF (Abaskohi et al., 2023) to encourage lexical and syntactic variation while preserving task semantics and avoiding hallucinated or omitted requirements.

Representative example Below is a representative example from the “Big Data Visualization Platform” task. Although the wording changes substantially across P_1 – P_4 , the functional requirements remain invariant.

- **Base Prompt (P_0):** “Please implement a big data visualization platform for data analysis and display. The platform should have functionalities for data visualization, report editing, dashboard preview, resource tree management, text editing, and data analysis. Users should be able to log in, browse data, edit reports, preview dashboards, manage resource trees, edit text, and perform data analysis. Use light salmon for the background and coral for components.”
- **Rephrasing 1 (P_1):** “Create a platform for big data visualization and analysis. It must include features for editing reports, viewing dashboards, managing resource trees, and editing text. Users should be able to log in, explore data, and analyze it. Set the background to light salmon and components to coral.”
- **Rephrasing 2 (P_2):** “Develop a big data analysis and display system. Key functions should be data visualization, report creation, dashboard previews, and resource management. Users need to log in to browse data and perform analyses. Use light salmon for the background color and coral for the elements.”
- **Rephrasing 3 (P_3):** “I need a solution for visualizing and analyzing big data. The system should allow users to log in, manage resources, edit text and reports, and preview dashboards. The design must use a light salmon background with coral-colored components.”
- **Rephrasing 4 (P_4):** “Construct a web platform dedicated to big data visualization. Features include report editing, data analysis, and dashboard previews. Users must be able to log in and manage data. The UI should feature a light salmon background and coral components.”

This separation of semantic invariants from surface wording allows us to test whether insecure generations are robust failure modes or artifacts of a particular phrasing.

D.3. FSTab Attack Evaluation

D.3.1. FULL WEBGENBENCH ATTACK RESULTS

Table D.3.1 reports the full per-domain attack table that was removed from the main paper in favor of a compact domain-averaged summary.

Extracting Recurring Vulnerabilities from Black-Box LLM-Generated Software

Table 10. Overlap-based prediction performance on the WebGenBench dataset. We report CodeQL and Semgrep results for ASR and ACR (%). ASR denotes at-least-one overlap with the scanner findings. Values are presented as CodeQL — Semgrep.

Model	E-commerce		Internal Tools		Social Media		Blogging		Dashboards	
	ASR ↑	ACR ↑	ASR ↑	ACR ↑	ASR ↑	ACR ↑	ASR ↑	ACR ↑	ASR ↑	ACR ↑
<i>Held-out (target-domain) evaluation</i>										
GPT-5.2	100 — 100	100 — 86.67	60 — 75	60 — 75	80 — 75	70 — 52.50	80 — 80	80 — 65	100 — 100	100 — 100
Claude-4.5 Opus	100 — 100	100 — 100	50 — 60	50 — 60	75 — 80	75 — 77.50	100 — 100	100 — 100	100 — 100	100 — 100
Gemini-3 Pro	100 — 100	100 — 100	40 — 60	40 — 44	60 — 80	60 — 66.67	80 — 80	80 — 80	100 — 100	100 — 100
Gemini-3 Flash	100 — 100	100 — 100	25 — 60	25 — 35	50 — 66.67	50 — 66.67	100 — 100	100 — 100	25 — 50	25 — 50
Composer	100 — 100	100 — 100	50 — 60	50 — 57.14	75 — 75	50 — 75	66.67 — 75	50 — 75	100 — 100	100 — 100
Grok	100 — 100	100 — 81.82	33.33 — 50	33.33 — 50	75 — 80	62.50 — 60.61	75 — 60	75 — 57.14	100 — 75	100 — 75
<i>Cross-domain evaluation</i>										
GPT-5.2	76.47 — 81.25	74.23 — 70.97	88.24 — 87.50	83.82 — 75	80.65 — 87.50	80.65 — 80	80.65 — 87.50	77.94 — 77.78	78.57 — 83.33	76.47 — 69.57
Claude-4.5 Opus	72.73 — 81.25	72.73 — 80	90 — 93.75	90 — 93.33	80 — 87.50	80 — 87.50	76.92 — 84.62	76.92 — 84	75 — 81.25	75 — 80
Gemini-3 Pro	61.54 — 75	61.54 — 65.52	80.77 — 87.50	80.77 — 83.33	75 — 81.25	75 — 76.47	69.23 — 81.25	69.23 — 72	70 — 80	70 — 73.33
Gemini-3 Flash	50 — 66.67	50 — 56.25	80 — 75	80 — 75	57.14 — 70	57.14 — 57.14	42.86 — 63.64	42.86 — 52	55.56 — 72.73	55.56 — 61.54
Composer	68.75 — 76.19	58.33 — 75	83.33 — 87.50	71.43 — 87.50	75 — 81.82	71.43 — 81.25	76.92 — 81.82	69.23 — 81.25	71.43 — 76.19	61.11 — 75
Grok	68.75 — 66.67	65 — 60.71	85 — 78.57	81 — 68.18	75 — 72.22	75 — 66.67	75 — 77.78	71.43 — 66.67	71.43 — 74.07	68.18 — 62.50

D.3.2. REPRESENTATIVE CLAUDE-4.5 OPUS FSTAB

Table 11 contains the Claude-specific FSTab that was removed from the main paper.

Table 11. Representative model-specific FSTab for Claude-4.5 Opus.

Feature	Top Recurring Vulnerabilities	Feature	Top Recurring Vulnerabilities
Access Admin Panel	js/missing-rate-limiting	Manage User Permissions	js/missing-rate-limiting
Apply Search Filter	py/flask-debug, js/missing-rate-limiting	Register New Account	js/clear-text-storage..., js/missing-rate-limiting
Browse Product Catalog	js/missing-rate-limiting	Reset Forgotten Password	js/missing-rate-limiting
Create Backup	py/path-injection	Save New Record To DB	py/sql-injection, py/stack-trace-exposure
Delete Record From DB	py/stack-trace-exposure, js/missing-rate-limiting	Update Record In DB	js/missing-rate-limiting
Download File	py/path-injection, py/flask-debug	Upload Document or File	py/stack-trace-exposure, js/xss-through-dom
Fetch Data From DB	js/xss-through-dom, py/stack-trace-exposure	User Login (Password)	js/remote-prop-injection, js/insecure-random
Follow User	js/regex/missing-regex-anchor	User Login (Social)	js/missing-rate-limiting
Gen/Validate Auth Token	js/missing-rate-limiting	View Analytics Dashboard	js/missing-rate-limiting
Like Or Upvote Content	js/missing-rate-limiting	View Order Status	js/missing-rate-limiting
Load Next Page	js/regex/missing-anchor, js/missing-rate-limiting	View User Profile	js/missing-rate-limiting

D.3.3. FSTAB: MODEL-SPECIFIC VULNERABILITY DATABASES

This subsection provides the remaining model-specific FSTab lookup mappings for the evaluated production models. Together with Table 11, these tables summarize the feature-conditioned vulnerability databases used in our attack analysis. To ensure conciseness, we display only features where at least one recurring vulnerability pattern was identified during construction.

Table 12. FSTab: Recurring Vulnerability Fingerprints for GPT-5.2.

feature	Top Recurring Vulnerabilities (Rule IDs)
Access Admin Panel	js/missing-rate-limiting
Add Item To Shopping Cart	js/remote-property-injection, py/url-redirectation
Apply Search Filter	js/missing-origin-check, js/missing-rate-limiting
Delete Record From Database	py/url-redirectation
Download File	js/remote-property-injection, py/path-injection
Fetch Data From Database	py/path-injection
Import Data From File	py/sql-injection
Load Next Page	js/regex/missing-regexp-anchor, py/sql-injection
Manage User Permissions	py/url-redirectation
Publish New Post	js/missing-rate-limiting
Register New Account	js/prototype-pollution-utility, js/missing-rate-limiting
Submit Payment	py/url-redirectation
Update Record In Database	py/url-redirectation, js/missing-rate-limiting
Upload Document Or File	py/path-injection
User Login With Password	js/client-side-unvalidated-url-redirectation, js/xss
View Inbox Messages	js/missing-rate-limiting
View User Profile	js/missing-rate-limiting

Table 13. FSTab: Recurring Vulnerability Fingerprints for Gemini-3 Pro.

feature	Top Recurring Vulnerabilities (Rule IDs)
Add Item To Shopping Cart	py/flask-debug
Apply Search Filter	py/flask-debug
Block User	js/xss-through-dom
Create Backup	py/path-injection
Manage User Permissions	py/flask-debug
Register New Account	py/flask-debug
Save New Record To Database	py/url-redirectation
User Login With Password	js/xss, js/client-side-unvalidated-url-redirectation
User Logout	py/flask-debug

Table 14. FSTab: Recurring Vulnerability Fingerprints for Gemini-3 Flash.

feature	Top Recurring Vulnerabilities (Rule IDs)
Access Admin Panel	js/missing-rate-limiting
Apply Search Filter	py/flask-debug
Generate Or Validate Auth Token	js/missing-rate-limiting
Register New Account	js/missing-rate-limiting
Upload Document Or File	py/stack-trace-exposure, py/url-redirectation
User Login With Password	py/flask-debug, js/missing-rate-limiting
View User Profile	js/missing-rate-limiting

Extracting Recurring Vulnerabilities from Black-Box LLM-Generated Software

Table 15. FSTab: Recurring Vulnerability Fingerprints for Composer.

feature	Top Recurring Vulnerabilities (Rule IDs)
Access Admin Panel	js/missing-rate-limiting
Apply Search Filter	py/flask-debug,py/sql-injection
Block User	js/xss-through-dom
Create Backup	py/path-injection,py/stack-trace-exposure
Delete Record From Database	py/path-injection,py/stack-trace-exposure
Download File	py/path-injection,py/stack-trace-exposure
Fetch Data From Database	js/request-forgery,py/stack-trace-exposure
Generate Or Validate Auth Token	js/missing-rate-limiting
Like Or Upvote Content	js/missing-rate-limiting
Load Next Page	js/missing-rate-limiting
Manage User Permissions	js/missing-rate-limiting
Post Comment	js/missing-rate-limiting
Register New Account	js/sql-injection,js/missing-rate-limiting
Save New Record To Database	py/stack-trace-exposure,js/missing-rate-limiting
Search Content	js/missing-rate-limiting
Send Invitation	js/missing-rate-limiting
Share Content	js/missing-rate-limiting
Sort Results	js/sql-injection,py/flask-debug
Submit Payment	js/missing-rate-limiting
Update Record In Database	js/missing-rate-limiting
Upload Document Or File	py/stack-trace-exposure,js/missing-rate-limiting
User Login With Password	js/prototype-polluting-assignment,js/remote-property-injection
User Login With Social Account	js/missing-rate-limiting
View Analytics Dashboard	js/missing-rate-limiting
View Inbox Messages	js/missing-rate-limiting
View Order Status	js/sql-injection,js/missing-rate-limiting
View Shopping Cart	js/missing-rate-limiting
View User Profile	js/missing-rate-limiting

1131
1132
1133
1134
1135
1136
1137
1138
1139
1140
1141
1142
1143
1144
1145
1146
1147
1148
1149
1150
1151
1152
1153
1154

Table 16. FSTab: Recurring Vulnerability Fingerprints for Grok.

feature	Top Recurring Vulnerabilities (Rule IDs)
Access Admin Panel	py/stack-trace-exposure
Apply Search Filter	py/flask-debug, py/stack-trace-exposure
Block User	js/functionality-from-untrusted-source
Create Backup	py/log-injection, py/stack-trace-exposure
Delete Record From Database	py/path-injection, py/stack-trace-exposure
Download File	py/path-injection
Fetch Data From Database	py/sql-injection, js/xss-through-dom
Generate Or Validate Auth Token	js/sql-injection, js/missing-rate-limiting
Like Or Upvote Content	js/missing-rate-limiting
Load Next Page	js/remote-property-injection, js/sql-injection
Proceed To Checkout	py/flask-debug
Register New Account	py/flask-debug, js/missing-rate-limiting
Save New Record To Database	js/sql-injection, py/stack-trace-exposure
Search Content	js/sql-injection
Sort Results	js/missing-rate-limiting
Submit Payment	js/missing-rate-limiting
Update Record In Database	js/sql-injection, py/stack-trace-exposure
Upload Document Or File	py/url-redirectation, py/path-injection
User Login With Password	js/redos, js/clear-text-storage-of-sensitive-data
View Analytics Dashboard	js/missing-rate-limiting, py/stack-trace-exposure
View Inbox Messages	js/missing-rate-limiting
View Order Status	js/missing-rate-limiting
View Shopping Cart	js/missing-rate-limiting
View User Profile	js/missing-rate-limiting, js/sql-injection

D.4. Tables

D.4.1. CONSTRUCTION-BUDGET ABLATION

The construction-budget ablation was removed from the main paper for space. Figure 6 and Figure 7 show that both ASR and ACR plateau around 20 construction projects, which motivates our default budget choice.

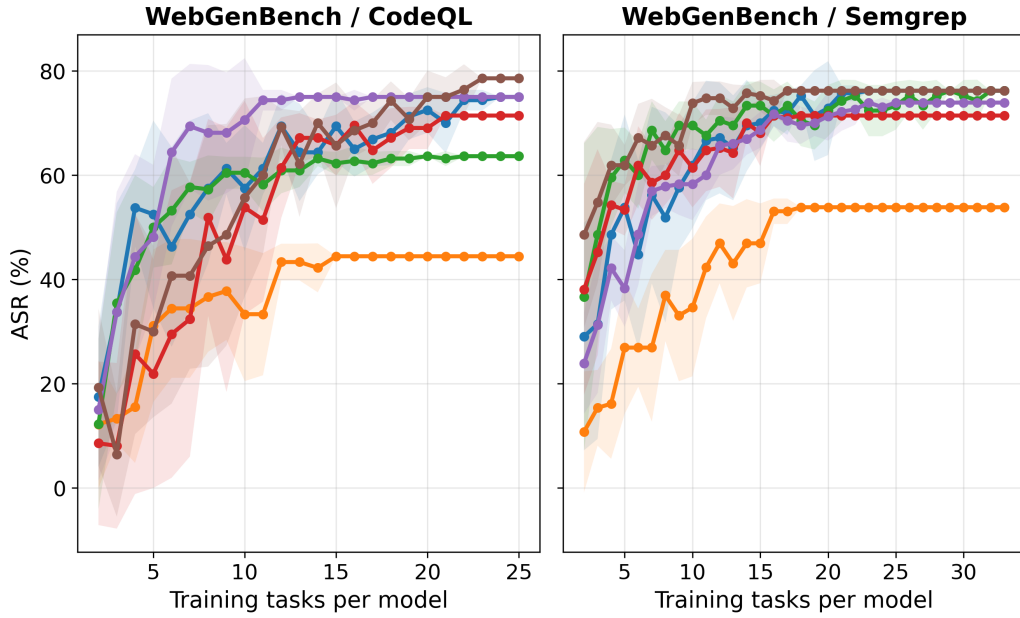


Figure 6. ASR vs. construction budget (WebGenBench, FSTab with $N=1$). Both benchmarks plateau around 20 projects.

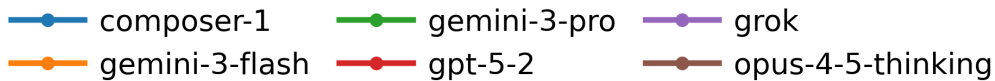
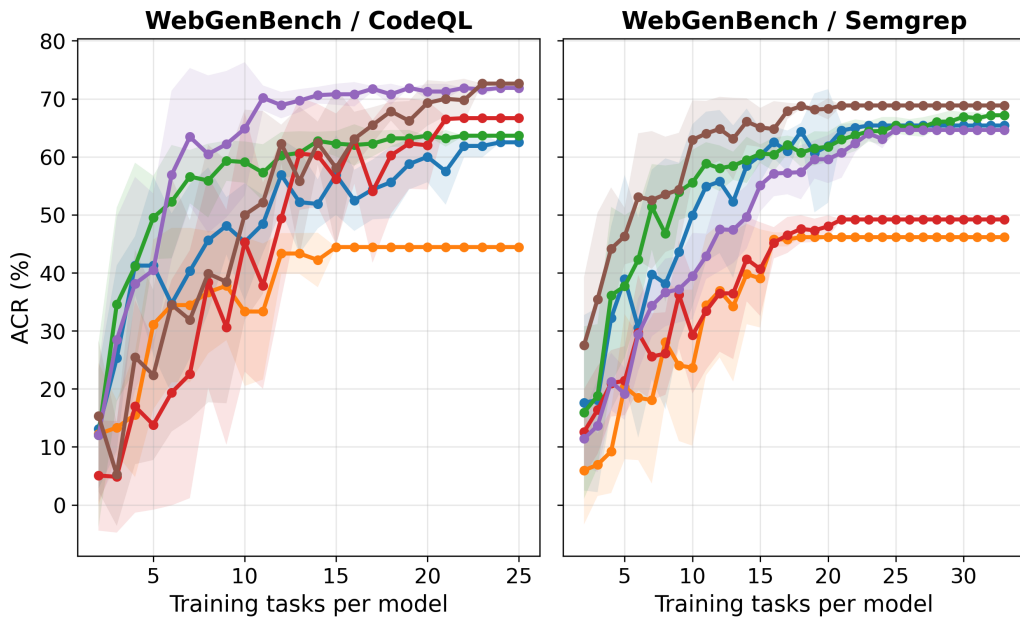


Figure 7. ACR vs. construction budget under the same sweep. The plateau near 20 projects motivates our construction budget choice.

D.4.2. ATTACK RULE BUDGET AND CWE COVERAGE

Because FSTab relies on a minimum-support threshold to filter noise, it learns only a tightly bounded space of the most recurring vulnerabilities. In our construction pipeline, we retain only feature–rule pairs observed at least three times ($C(f, r) \geq 3$). This yields 28 learnable CodeQL rules and 39 learnable Semgrep rules, even though the underlying scanners expose 300+ and 5,000+ rules, respectively. After deduplicating repeated rule IDs across the feature-conditioned query results for a target program, the average prediction set remains small: 4.86 CodeQL rules per project and 8.03 Semgrep rules per project. The resulting coverage still spans critical vulnerabilities families such as CWE-89 (SQL Injection), CWE-79 (Cross-Site Scripting), CWE-22 (Path Traversal), and CWE-20 (Improper Input Validation).

Table 17. R6: CWE coverage summary for the bounded FSTab rule budget.

Statistic	CodeQL	Semgrep
Learnable rules	28	39
Distinct CWE IDs	40	22
Total scanner rules	300+	5,000+
Avg. rules/project	4.86	8.03

This bounded budget matters operationally. An external auditor can realistically inspect 5-8 high-priority rules per project; triaging thousands of generic scanner alerts is not feasible. The results therefore show that recurrence is not only statistically measurable, but practically usable.

Representative CodeQL coverage includes CWE-89 (SQL Injection), CWE-79 (Cross-Site Scripting), CWE-770 (Missing Rate Limiting), CWE-601 (Open Redirect), CWE-22/CWE-23/CWE-73 (Path Traversal variants), CWE-338 (Weak Randomness), CWE-730/CWE-1333 (ReDoS), CWE-312/CWE-315 (Cleartext Storage), CWE-209 (Stack Trace Exposure), CWE-918 (SSRF), CWE-807 (Authentication Bypass), CWE-94 (Code Injection), CWE-400 (Resource Exhaustion), CWE-489 (Debug Mode), CWE-434 (Unrestricted Upload), and CWE-307 (Brute Force), among others.

Representative Semgrep coverage includes CWE-352 (CSRF), CWE-522/CWE-798 (Hardcoded Credentials), CWE-79 (XSS), CWE-89 (SQL Injection), CWE-489 (Debug Mode), CWE-521 (Weak Password), CWE-601 (Open Redirect), CWE-942 (CORS Misconfiguration), CWE-502 (Deserialization), CWE-319 (Cleartext Transmission), CWE-1333 (ReDoS), CWE-22 (Path Traversal), and CWE-250 (Unnecessary Privileges), among others.

D.4.3. EXHAUSTIVE FEATURE LEVEL VULNERABILITY RECURRENCE (FVR)

This subsection provides the exhaustive feature-level Vulnerability Recurrence (FVR) scores for each of the six evaluated production models. The FVR score represents the stability of vulnerability patterns for a given feature. Values closer to 100 indicate high persistence in the model’s security failures for that specific feature.

Table 18. FVR Scores: Active User Lifecycle and Security Triggers.

Model	Register Account ↑	User Login (Password) ↑	User Logout ↑	Generate Auth Token ↑
GPT-5.2	100.00	40.91	0.00	0.00
Claude-4.5 Opus	66.67	52.94	0.00	50.00
Gemini-3 Pro	100.00	71.43	100.00	0.00
Gemini-3 Flash	100.00	60.00	0.00	100.00
Composer	40.00	60.87	0.00	50.00
Grok	100.00	68.42	0.00	100.00

Extracting Recurring Vulnerabilities from Black-Box LLM-Generated Software

Table 19. FVR Scores: Active Database and Persistence Triggers.

Model	Delete Record ↑	Save New Record ↑	Update Record ↑	Fetch Data ↑	Create Backup ↑
GPT-5.2	100.00	25.00	40.00	20.00	0.00
Claude-4.5 Opus	40.00	57.14	25.00	33.33	0.00
Gemini-3 Pro	0.00	66.67	0.00	0.00	0.00
Gemini-3 Flash	0.00	0.00	0.00	0.00	0.00
Composer	100.00	40.00	50.00	50.00	33.33
Grok	25.00	28.57	66.67	33.33	20.00

Table 20. FVR Scores: Active UI and Search Interaction Triggers.

Model	Handle UI Event ↑	Toggle UI Elem. ↑	Load Next Pg ↑	Apply Filter ↑	Sort Results ↑
GPT-5.2	100.00	0.00	75.00	40.00	100.00
Claude-4.5 Opus	0.00	0.00	50.00	60.00	33.33
Gemini-3 Pro	0.00	0.00	50.00	100.00	100.00
Gemini-3 Flash	0.00	0.00	0.00	20.00	0.00
Composer	66.67	66.67	40.00	75.00	100.00
Grok	0.00	0.00	50.00	80.00	100.00

Table 21. FVR Scores: Active System Integration and Middleware Triggers.

Model	API Request ↑	Websocket Conn. ↑	Process Mid.ware ↑	Init. App ↑	Run Test ↑
GPT-5.2	66.67	0.00	0.00	33.33	0.00
Claude-4.5 Opus	75.00	33.33	0.00	37.50	50.00
Gemini-3 Pro	100.00	50.00	0.00	50.00	50.00
Gemini-3 Flash	50.00	0.00	0.00	66.67	100.00
Composer	80.00	100.00	100.00	40.00	0.00
Grok	50.00	60.00	100.00	50.00	0.00

Table 22. FVR Scores: Active Social Engagement and Publishing Triggers.

Model	Like/Upvote Content ↑	Follow User ↑	Block User ↑	Publish New Post ↑	Edit Exist. Post ↑
GPT-5.2	0.00	0.00	0.00	100.00	0.00
Claude-4.5 Opus	100.00	50.00	0.00	0.00	0.00
Gemini-3 Pro	100.00	0.00	100.00	100.00	100.00
Gemini-3 Flash	100.00	0.00	0.00	100.00	0.00
Composer	33.33	0.00	50.00	0.00	0.00
Grok	100.00	0.00	33.33	0.00	0.00

Table 23. FVR Scores: Active File Handling and Download Triggers.

Model	Download File ↑	Upload Doc/File ↑	Share Content ↑
GPT-5.2	60.00	50.00	0.00
Claude-4.5 Opus	100.00	50.00	50.00
Gemini-3 Pro	0.00	50.00	0.00
Gemini-3 Flash	0.00	33.33	0.00
Composer	80.00	66.67	50.00
Grok	50.00	37.50	0.00

Table 24. FVR Scores: Active Administrative and Platform Control Triggers.

Model	Admin Panel ↑	User Perms ↑	Manage Users ↑	Analytics Dash ↑
GPT-5.2	50.00	0.00	0.00	0.00
Claude-4.5 Opus	100.00	100.00	0.00	0.00
Gemini-3 Pro	0.00	100.00	0.00	0.00
Gemini-3 Flash	100.00	0.00	0.00	0.00
Composer	50.00	100.00	0.00	0.00
Grok	0.00	0.00	100.00	50.00

Table 25. FVR Scores: Active Content Views and Transactional Triggers.

Model	View Inbox Messages ↑	View Order Status ↑	View Shopping Cart ↑	View Calendar ↑	Add To Cart ↑
GPT-5.2	100.00	0.00	0.00	0.00	25.00
Claude-4.5 Opus	0.00	100.00	0.00	100.00	0.00
Gemini-3 Pro	0.00	0.00	0.00	0.00	100.00
Gemini-3 Flash	0.00	0.00	0.00	0.00	0.00
Composer	100.00	100.00	100.00	100.00	0.00
Grok	50.00	0.00	0.00	50.00	0.00

Table 26. FVR Scores: Active Commerce Workflows and Multi-Agent Utilities.

Model	Proceed To Checkout ↑	Submit Payment ↑	Login Generic ↑	Post Comment ↑	Utility Helper ↑
GPT-5.2	0.00	0.00	100.00	0.00	0.00
Claude-4.5 Opus	0.00	0.00	50.00	0.00	0.00
Gemini-3 Pro	0.00	0.00	100.00	0.00	0.00
Gemini-3 Flash	0.00	0.00	0.00	0.00	0.00
Composer	0.00	25.00	33.33	50.00	50.00
Grok	50.00	33.33	66.67	0.00	0.00

D.4.4. EXHAUSTIVE REPHRASING VULNERABILITY PERSISTENCE (RVP)

This subsection provides a prompt-slot diagnostic view of the rephrasing experiment. The formal aggregate metric RVP_{model} is defined in Section C.3 and averages recurrence jointly across all five realizations of each task. Table 27, by contrast, breaks the same experiment out by prompt slot: P0 denotes the original prompt, and P1–P4 denote the four semantic-preserving

rewrites. The goal is to show whether persistence is roughly uniform across prompt realizations or disproportionately driven by particular prompt slots, rather than to redefine RVP itself.

Table 27. RVP Scores across Prompt Variations (CodeQL Only, %)

Model	P0 ↑	P1 ↑	P2 ↑	P3 ↑	P4 ↑
GPT-5.2	49.70	45.00	23.94	39.50	42.86
Claude-4.5 Opus	32.95	66.96	54.28	32.98	37.69
Gemini-3 Pro	31.16	44.93	53.79	40.91	53.57
Gemini-3 Flash	31.67	23.70	83.33	47.50	55.00
Composer	49.98	53.29	54.92	52.73	56.43
Grok	23.68	30.37	24.91	17.48	36.82

D.4.5. EXHAUSTIVE DOMAIN RECURRENCE AND TRANSFER (DVR & CDT)

The following tables present the Within-Domain Recurrence (DVR) and Cross-Domain Transfer (CDT) scores. High CDT scores indicate that vulnerability patterns generalize across disparate application domains.

Table 28. Domain Vulnerability Recurrence (DVR) Scores (CodeQL Only, %)

Model	E-Commerce ↑	Publishing ↑	Social ↑	Analytics ↑	Internal ↑
GPT-5.2	46.67	21.21	34.62	28.00	39.13
Claude-4.5 Opus	48.78	37.50	13.89	30.00	28.57
Gemini-3 Pro	33.33	47.06	44.44	40.00	42.11
Gemini-3 Flash	37.50	26.32	50.00	25.00	41.67
Composer	50.94	50.00	44.23	43.59	43.40
Grok	37.04	25.00	29.55	25.45	22.22

Table 29. Cross-Domain Vulnerability Transfer (CDT) Scores (CodeQL Only, %)

Model	E-Commerce ↑	Publishing ↑	Social ↑	Analytics ↑	Internal ↑
GPT-5.2	73.33	39.39	26.92	24.00	47.83
Claude-4.5 Opus	53.66	55.00	41.67	64.52	53.06
Gemini-3 Pro	60.00	82.35	55.56	53.33	42.11
Gemini-3 Flash	87.50	47.37	37.50	33.33	58.33
Composer	56.60	70.59	50.00	64.10	45.28
Grok	55.56	62.50	59.09	57.14	52.17

E. E2EDev Attack Performance

Table 30 presents the detailed ASR and ACR results for the E2EDev dataset across all models and domains, where ASR denotes at-least-one overlap with the scanner findings. Values are presented as CodeQL / Semgrep. Relative to WebGenBench, the performance drop on E2EDev is driven primarily by feature sparsity rather than by a contradiction of the recurrence hypothesis. E2EDev prompts intentionally describe smaller applications, and the resulting projects expose only 2.5 extracted UI features per project on average, compared with 8.6 on WebGenBench. Because FSTab is trained on WebGenBench-style programs, E2EDev constitutes a genuine out-of-distribution transfer setting.

Table 30. Overlap-based prediction performance on the E2EDev dataset. We report CodeQL and Semgrep results for ASR and ACR (in %), where ASR denotes at-least-one overlap with the scanner findings. Values are presented as CodeQL / Semgrep.

Model	E-commerce		Internal Tools		Social Media		Blogging		Dashboards	
	ASR ↑	ACR ↑	ASR ↑	ACR ↑	ASR ↑	ACR ↑	ASR ↑	ACR ↑	ASR ↑	ACR ↑
<i>Held-out (target-domain) evaluation</i>										
GPT-5.2	- / 0	- / 0	100 / 33.33	100 / 33.33	0 / 100	0 / 100	100 / 75	100 / 75	100 / 50	100 / 50
Claude-4.5 Opus	100 / 0	100 / 0	50 / 100	50 / 100	0 / 100	0 / 100	100 / 100	100 / 100	0 / 50	0 / 50
Gemini-3 Pro	100 / 100	100 / 100	33.33 / 33.33	33.33 / 33.33	100 / 100	100 / 100	100 / 75	100 / 75	100 / 100	100 / 100
Gemini-3 Flash	100 / 100	100 / 100	100 / 50	100 / 50	100 / 100	100 / 100	100 / 75	100 / 75	100 / 66.67	100 / 66.67
Composer	- / 0	- / 0	50 / 50	50 / 50	0 / 100	0 / 100	100 / 50	100 / 50	0 / 0	0 / 0
Grok	100 / 100	100 / 100	- / 50	- / 50	0 / 100	0 / 100	100 / 50	100 / 50	100 / 100	100 / 100
<i>Cross-domain evaluation</i>										
GPT-5.2	75 / 63.64	75 / 63.64	66.67 / 66.67	66.67 / 66.67	100 / 50	100 / 50	66.67 / 50	66.67 / 50	66.67 / 60	66.67 / 60
Claude-4.5 Opus	40 / 90.91	40 / 90.91	50 / 77.78	50 / 77.78	60 / 77.78	60 / 77.78	40 / 77.78	40 / 77.78	60 / 90	60 / 90
Gemini-3 Pro	71.43 / 72.73	71.43 / 72.73	100 / 88.89	100 / 88.89	75 / 70	75 / 70	71.43 / 75	71.43 / 75	75 / 70	75 / 70
Gemini-3 Flash	83.33 / 66.67	83.33 / 66.67	100 / 71.43	100 / 71.43	75 / 58.33	75 / 58.33	66.67 / 63.64	66.67 / 63.64	75 / 57.14	75 / 57.14
Composer	50 / 54.55	50 / 54.55	66.67 / 66.67	66.67 / 66.67	60 / 70	60 / 70	50 / 57.14	50 / 57.14	60 / 50	60 / 50
Grok	75 / 72.73	75 / 72.73	60 / 70	60 / 70	75 / 66.67	75 / 66.67	66.67 / 66.67	66.67 / 66.67	75 / 66.67	75 / 66.67

F. Statistical Significance Summary

For the held-out WebGenBench attack comparison, we report 95% Wilson confidence intervals (closed-form binomial, with no Normality assumption) on aggregate ASR over project-model evaluation units. We do not report corresponding Wilson intervals for E2EDev. For stochastic experiments: Random-Budget sampling, wrong-fingerprint pairing, and label-noise perturbations. We report the 1σ sample standard deviation across 10 independent random seeds.

Table 31. Aggregate held-out WebGenBench ASR with 95% Wilson confidence intervals over project-model evaluation units. The non-overlapping intervals show a clean separation between FSTab and the matched-budget Random-Budget baseline.

Eval	FSTab ASR	Random-Budget ASR
WebGen CodeQL	69.4% [59.7–77.6]	9.4% [4.4–17.4]
WebGen Semgrep	72.5% [63.9–79.7]	20.8% [14.5–28.6]

Table 32. Seed variation for stochastic robustness experiments. Values report 1σ sample standard deviation over 10 independent random seeds.

Experiment	Seed std (1σ over 10 seeds)
Random-Budget	ASR \pm 2.3–2.6 pts
Wrong-fingerprint	ASR \pm 1.6–1.9 pts
Label-noise (drop / add / swap)	ASR \pm 0.6–2.3 pts
Rule-frequency tail-only	ASR \pm 3.5–6.0 pts

G. Static Analysis Validation

To rigorously assess the fidelity of our automated ground-truth generation, we implemented a human-in-the-loop validation protocol on a randomly sampled subset of the generated projects. The objective was to quantify the rate of false positives in our static analysis pipeline and ensure that the recurrence metrics report actionable security flaws rather than tool artifacts.

1540 **Methodology** We performed a manual code audit on the sampled projects, specifically verifying the exploitability and
1541 reachability of vulnerabilities flagged by our dual-engine scanner (CodeQL and Semgrep). For each flagged instance, a
1542 human expert reviewed the generated source code to determine if the detected pattern constituted a genuine violation of the
1543 associated CWE definition (True Positive) or just harmless code (False Positive).
1544

1545 **Precision Analysis** Our audit revealed precision rates of **82%** for CodeQL and **74%** for Semgrep. While static analysis
1546 always misses some nuance, these scores show that the majority of flagged items are actual insecure coding patterns.
1547 Furthermore, since FSTab focuses on comparing rates between models rather than counting total vulnerabilities, these
1548 validation rates suggest our metrics are conservative. The fact that both scanners found consistent patterns confirms that
1549 findings like the “Universality Gap” come from the models themselves, not from errors in a specific tool.
1550
1551
1552
1553
1554
1555
1556
1557
1558
1559
1560
1561
1562
1563
1564
1565
1566
1567
1568
1569
1570
1571
1572
1573
1574
1575
1576
1577
1578
1579
1580
1581
1582
1583
1584
1585
1586
1587
1588
1589
1590
1591
1592
1593
1594

H. Semantic Feature Extraction Example

This section provides a concrete, end-to-end example of how our automated pipeline assigns an observable frontend feature (a semantic UI action) to a specific code location. The example follows the procedure in Section C.1: (i) isolate the enclosing code context around a target line and (ii) score candidate actions using the heuristic relevance function $S(a, C_\ell)$, assigning $\hat{a} = \arg \max_a S(a, C_\ell)$.

H.1. Example Setup: JavaScript WebSocket Chat Handler

Input We consider a client-side JavaScript file in a chat plugin that supports sending messages and sharing files. A static analyzer flags a finding at line $\ell = 17$ (file-link construction in the WebSocket receive handler). The feature extractor is given the pair (file path, line number) and returns a semantic UI action label.

Local code context The following snippet shows the relevant lines (the context window used by the extractor includes the full `ws.onmessage` handler surrounding the target line):

```

14: } else if (data.type === 'file') {
15:     messageDiv.classList.add('received');
16:     var link = document.createElement('a');
17:     link.href = data.url;
18:     link.className = 'file-link';
19:     link.target = '_blank';
20:     link.innerHTML = 'Clip: ' + data.filename;
    
```

H.2. Step 1: Structural Context Extraction

For JavaScript/TypeScript, the pipeline identifies the enclosing functional unit and lightweight API cues. In this case, the target line is inside a WebSocket message-receive callback (`ws.onmessage`), so we treat the enclosing handler body as C_ℓ .

Extracted evidence (illustrative) From C_ℓ , we collect a small set of signals: (i) function/event handler name (e.g., `onmessage`), (ii) salient identifiers (e.g., `messages`, `messageDiv`, `data`, `filename`, `url`), (iii) string literals (e.g., "message", "file", "file-link"), and (iv) API-pattern matches indicating a WebSocket workflow (e.g., `new WebSocket / onmessage`).

H.3. Step 2: Candidate Action Scoring

Let A denote the taxonomy of semantic UI actions (Section C.1.1). For each candidate action $a \in A$, we compute a relevance score $S(a, C_\ell)$ as in Eq. 11, aggregating evidence from function names, identifiers, string literals, route tokens (if present), and API-pattern matches, with caps on identifier/string contributions.

Two competing candidates In this snippet, the code touches both *messaging* and *file sharing*. We highlight two plausible candidates:

- `SENDCHATMESSAGE`: messaging/real-time chat interaction.
- `UPLOADDOCUMENTORFILE`: file transfer functionality.

Score for `SendChatMessage` The WebSocket receive handler name and the presence of message-centric identifiers provide strong evidence, augmented by an API-pattern match for WebSockets. Using the calibrated weights from Section C.1 and the identifier cap τ_{id} , the contributions (illustratively) sum to:

$$\begin{aligned}
 S(\text{SENDCHATMESSAGE}, C_\ell) &\approx w_{fn} \cdot 1 + \min(\tau_{id}, w_{id} \cdot \#(\text{message identifiers})) \\
 &\quad + \min(\tau_{str}, w_{str} \cdot \#(\text{message strings})) + w_{api} \cdot 1 \\
 &= 2.5 + 1.5 + 0.35 + 1.8 = 6.15.
 \end{aligned} \tag{31}$$

Score for UploadDocumentOrFile Although file-related tokens appear (`file`, `filename`, `href`), they constitute weaker support under the same weighting scheme:

$$S(\text{UPLOADDOCUMENTORFILE}, C_\ell) \approx w_{\text{id}} \cdot 1.0 + w_{\text{str}} \cdot 1 = 0.5 + 0.35 = 0.85.$$

H.4. Step 3: Feature Assignment and Output Record

The extractor assigns

$$\hat{a} = \arg \max_{a \in A} S(a, C_\ell) = \text{SENDCHATMESSAGE},$$

and outputs a compact record attached to the static-analysis finding, e.g., `ui_action = send_chat_message` and `ui_action_confidence = 6.15`. In our pipeline, this assignment is performed only when $S(\hat{a}, C_\ell)$ exceeds a small threshold (default: 0.0), to avoid spurious labels.

Interpretation Although computed from code for scalability in our evaluation, the extracted feature corresponds to a *black-box observable* user intent: a site with a chat interface that receives/displays messages and shared items. This is precisely the semantic level at which FSTab operates (feature \rightarrow likely backend rule IDs), without requiring access to backend code during inference.

Role in the threat model The source-level extraction shown here is used only to label attacker-owned construction data and to make the benchmark reproducible at scale. It is not required for the victim-facing attack. At deployment time, an auditor only needs to determine whether observable actions such as chat, login, search, upload, checkout, or admin access are present something that can be done manually or with ordinary UI interaction, DOM inspection, route discovery, and network tracing. We manually verified this correspondence across the evaluated models and domains, and found that the canonicalized frontend features align with the user-visible action set recoverable in this black-box manner. The paper’s contribution is the reusable feature-to-vulnerability table once those observable actions are known, not a new crawler or UI-semantic parser.

I. End-to-End Attack Demonstration Using FSTab (Case Study)

Goal We present an end-to-end case study showing how an attacker can leverage **FSTab** a model specific mapping from observable UI actions to likely backend vulnerability rule IDs to prioritize and validate exploitation paths in a black-box setting. This appendix is written for reproducibility and clarity, but follows a *responsible disclosure* style: we include measurement evidence and non-operational request skeletons, while omitting copy-pastable exploit payloads.

Target Our target is a full-stack web application (React frontend, Node/Express backend, MongoDB) generated by the `grok` model (“Smart Matrimonial Website”) as summarized in the accompanying report.

Threat model The attacker (i) can interact with the deployed UI and send HTTP requests to public endpoints, (ii) knows the source model identity m (here: `grok`), and (iii) has access to the corresponding FSTab T_m , but (iv) does *not* have access to backend source code.

I.1. From UI Reconnaissance to FSTab Query

Step 1: Extract observable UI actions Using black-box interaction with the UI, we identify high-confidence user-intent actions such as login, quick search, and advanced filtering. These correspond to our feature taxonomy entries and are the only inputs required to query FSTab. No source inspection is used in this step; the actions are identified from the victim’s visible interface alone.

Step 2: Query model-specific FSTab Table 33 shows the `grok`-specific top-ranked rule IDs returned for the extracted actions. Importantly, these predictions are *feature-conditioned* (e.g., search actions surface regex risks; auth actions surface rate-limiting / injection risks), and therefore provide a concrete triage list before any code inspection.

UI action (<i>f</i>)	Predicted rule ID (<i>r</i>)	Score	Confidence
user.login.with.password	js/sql-injection	0.427	Medium
user.login.with.password	js/regex-injection	0.367	Medium
apply.search.filter	js/missing-rate-limiting	-1.507	High
search.content	js/sql-injection	1.081	High
fetch.data.from.database	py/sql-injection	1.913	Very High

Table 33. FSTab query outputs used to guide triage in the case study (model: grok).

Case-specific prioritization Following the main-paper FSTab workflow, we prioritize (i) vulnerabilities reachable from the UI surface (search/auth), (ii) high-impact classes (auth bypass and DoS), and (iii) those consistent with the observed backend stack (Node/Mongo). The overall workflow is illustrated in the mapping-to-attack flow artifact.

I.2. Validated Attacks and Measured Evidence

I.2.1. ATTACK A: REGEX INJECTION: ReDOS (SEARCH)

Why this was selected Search-related UI actions strongly predicted `js/regex-injection` / `js/sql-injection` (Table 33), suggesting input-to-query risks. The report identifies vulnerable use of `new RegExp(userInput)` in search routes.

1760 **Vulnerable pattern (illustrative)**

```
1761
1762 if (location) query.location = new RegExp(location, 'i');
1763 if (occupation) query.occupation = new RegExp(occupation, 'i');
1764 const regex = new RegExp(searchQuery, 'i');
```

1766 **Measurement harness (non-operational)** To demonstrate impact without providing a copy-paste exploit, we use a timing harness that measures regex processing time as a function of adversarial input length (same structure as the provided script).

```
1769 // Pseudocode (sanitized): measure regex evaluation time
1770 for length in {10,15,20,25,30}:
1771   input = repeat("a", length) + "!"
1772   t_ms = time( RegExp(<redacted_pattern>).test(input) )
1773   log(length, t_ms)
```

1775 **Observed slowdown** Table 34 reports the measured latency increase: from sub-millisecond at length 10–15 to multi-second hangs at length 30 (DoS-scale).

Input length	Time (ms)	Observation
10	0.07	OK
15	0.24	OK
20	6.54	OK
25	208.26	Slowdown
30	6655.00	DoS-scale hang

1778 *Table 34.* ReDoS evidence from the local regex test log (search feature).

1788 I.2.2. ATTACK B: MISSING RATE LIMITING: CREDENTIAL STUFFING / BRUTE FORCE (AUTH)

1789 **Why this was selected** FSTab predicts `js/missing-rate-limiting` for multiple UI actions, and the mapping artifact highlights auth endpoints as critical targets.

1793 **Validation method** We run a rapid sequence of login requests and check whether the service returns HTTP 429 or otherwise throttles/blocks. The provided script explicitly tests for rate limiting by breaking on 429 and logging all attempts.

```
1796 # Pseudocode: rapid login attempts
1797 for i in 1..N:
1798   code = POST /api/auth/login with fixed email
1799   if code == 429: stop (rate limit triggered)
1800   else: log attempt i and code
```

1802 **Observed outcome** In the recorded run, requests were not blocked/throttled (attempts proceeded without a 429), consistent with missing rate limiting.

1805 I.2.3. ATTACK C: NOSQL INJECTION (AUTH) – PAYLOAD ACCEPTED, ENVIRONMENT-LIMITED VALIDATION

1807 **Why this was selected** FSTab prioritizes injection-class issues for auth/search actions (Table 33), and the analysis points to direct use of untrusted `email` values in Mongo queries.

1810 **Validation notes** We attempted operator-based injection through the login request body. In our deployment snapshot, the server returns a 500 with a MongoDB buffering timeout because the database service was not running, but the endpoint *accepts* the structured payload shape (i.e., it is not rejected by input validation), which is consistent with the predicted class. We therefore report this as **payload accepted / validation limited by environment** (rather than a confirmed auth bypass).

1815 **I.3. Summary and Mapping Quality (Single-Target Analogue)**

1816 **Attack outcomes** Across the three attack families above, we obtain: (i) a confirmed DoS-scale slowdown in search
1817 (ReDoS), (ii) confirmed absence of rate limiting on login attempts, and (iii) an injection attempt whose end-to-end impact
1818 is environment-limited but consistent with the predicted vulnerability class. The executive summary and flow artifacts
1819 summarize these results.
1820

1821 **Quantitative mapping signal** For this case study, the report summarizes an ASR of 100% and an ACR of 50%, meaning
1822 that the FSTab query overlapped the scanner-derived findings and covered 2/4 vulnerability types through mapping under
1823 the paper’s evaluation definitions.
1824

1825 **Severity (CVSS in report)** The report assigns high-to-critical severity to the demonstrated classes (e.g., NoSQL injection
1826 critical; ReDoS high), underscoring that FSTab-guided triage can surface practically meaningful risks early in the process.
1827

1828 **Responsible disclosure** We intentionally omit copy-pastable exploit payload strings and endpoint-specific exploit recipes
1829 in this appendix. Our goal is to demonstrate that *FSTab reduces attacker search cost* by converting UI-observable actions
1830 into actionable vulnerability hypotheses, validated via measurable outcomes (latency, throttling behavior, error modes),
1831 without turning the appendix into an operational exploitation manual.
1832